MESP2 AND TBX6 COOPERATIVELY ESTABLISH PERIODIC PATTERNS, COUPLED WITH THE CLOCK MACHINERY DURING MOUSE SOMITOGENESIS

MASAYUKI OGINUMA

DOCTOR OF PHILOSOPHY

DEPARTMENT OF GENETICS

SCHOOL OF LIFE SCENCE

THE GRADUATE UNIVERSITY FOR ADVANCED STUDIES

2007

Table of contents

Summary

The metameric structures in vertebrates are based on the periodicity of the somites that are formed one by one from the anterior end of the presomitic mesoderm (PSM) at the regular time. The timing of somitogenesis is regulated by the segmentation clock which is characterized by the oscillation of the Notch signaling pathways in mice. However, oscillation itself does not form a somite boundary. This temporal information has therefore to be accurately translated into a spatial pattern during somitogenesis. We have previously shown that Mesp2 is a crucial factor in this process. Mesp2 expression is periodically observed only in the anterior PSM, and the anterior border of the Mesp2 expression domain determines the next somite segmental border. However the nature of the spatio-temporal regulation and the link between Mesp2 and the segmentation clock has remained elusive.

In this study, I have employed high resolution fluorescent in situ hybridization in conjunction with immunohistochemical analyses of sections derived from single specimens and this has enabled us to determine the spatio-temporal relationship among several factors involved in mouse somitogenesis. I show here that the timing of Mesp2 expression is determined by the periodic waves of Notch activity and is spatially defined by Tbx6 in a way that *Mesp2* is induced in the region expressing Tbx6 protein. Interestingly, *Mesp2* mRNA initially shares an identical anterior border, but that once translated, the Mesp2 protein suppresses Tbx6 expression post-translationally. This reciprocal regulation is the spatial mechanism that successively defines the position of

the next anterior border of Mesp2. I also show that FGF signaling provides a spatial cue to position the posterior border of Mesp2.

Furthermore, to reveal the mechanism of post-translational Tbx6 suppression downstream of Mesp2, I tried to determine the domain of Tbx6 protein that was required for the suppression process. I generated transgenic mice harboring several types of Tbx6 protein that had truncation in several domains, under the control of endogenous promoter and enhancers of *Tbx6* using a BAC-base transgenic mouse technology. These results indicated that the T-box domain containing a DNA-binding motif, was essential and sufficient for the suppression of Tbx6 expression. In good agreement with these results, I found that Mesp2 also suppressed the expression of Brachyury, the other T-box factor protein, by the posttranslational mechanism.

Taken together, I conclude that Mesp2 is the final output signal by which the temporal information from the segmentation clock is translated to the segmental patterning, and reciprocal regulation between Mesp2 and Tbx6 create the periodic pattern during somitogenesis.

Introduction

During mouse embryogenesis, many morphogenetic events occur sequentially according to the scheduled time, indicating that these sequential events are linked with the precise temporal regulation. Such regulations must exist throughout embryogenesis to coordinate many developmental processes, although the molecular nature coordinating such temporal regulation is largely unknown.

The vertebrate body is subdivided into repeating segments along the anterior-posterior (AP) axis. This segmental or metameric pattern is established early in embryogenesis by the process of somitogenesis. Somites are blocks of paraxial mesoderm cells that give rise to the axial skeleton and their associated muscles and tendons, which retain a metameric pattern. During development, somitogenesis is tightly coupled with axis elongation. Precursors of the somites, called presomitic mesoderm (PSM), arise from the posterior end of embryo, called tail bud. Somites are aligned along the neural tube, and budding off from the anterior-most end of the unsegmented presomitic mesoderm at the regular time (Fig. 1). Interestingly, the intervals of each somite formation are different from species to species; 30 minutes in zebrafish, 90 minutes in chick, 2 hours in mouse, and 8 hours in human. Therefore, somitogenesis is an event that occurs according to the scheduled time, and it is believed that somitogenesis is under the precise control of temporal information(Dubrulle and Pourquie, 2002; Dubrulle and Pourquie, 2004a; Pourquie, 2003; Saga and Takeda, 2001).

In past decade, many people have proposed the model of the somitogenesis. Cooke and Zeeman devised the "clock & wavefront" model. The "clock & wavefront model" is an model that helps to explain the sequential generation of the somite with the interaction of two hypothetical elements, One is the intracellular oscillator, also called the clock, which determine the temporal periodicity of somitogenesis (Fig. 2A), and the other is the wavefront which determine the place of somitogenesis existing at the same distance from tail bud (Fig. 2B). The temporal periodicity created by the intracellular oscillator is translated into the spatial periodicity at the wavefront. Because PSM cells are supplied continually from the caudal region of the tail bud, regular space of segmentation is generated at the regular time in this model(Cooke and Zeeman, 1976).

In 1997, Palmeirim et al. provided a breakthrough with regard to an ultradian clock, by demonstrating an oscillatory expression of mRNA of the basic helix-loop-helix (bHLH) gene *chairy1*, a chick homologue of the Drosophila pair-rule gene *hairy*. Each cyclic expression is associated with somite segmentation. During somitogenesis, the expression of *chairy1* mRNA sweeps across the PSM anteriorly from the posterior end. This wave-like propagation is repeated synchronously with somite segmentation. This dynamic expression of *chairy1* is neither a result of cell movement nor periodically secreted diffusing signals but is the result of autonomous oscillation in gene expression that is synchronized among neighboring cells (Fig. 3B). These observations suggest that the segmentation clock is an intrinsic mechanism of the oscillatory gene expression in each PSM cell(Palmeirim et al., 1997).

In the recent studies, it was shown that Notch signaling is involved in the

segmentation clock. The expression of Notch downstream targets, such as *Hes7* (hairy and enhancer of split 7) and *Lfng* which encodes a glycosyltransferase that can modify Notch activity, oscillate in the PSM(Bessho et al., 2001; Evrard et al., 1998; McGrew et al., 1998). Mutations for *Lfng* and *Hes7* result in random and incomplete somite segmentation(Bessho et al., 2001; Evrard et al., 1998; Zhang and Gridley, 1998). Interestingly, constitutive expression of *Lfng* also disturbs somite segmentation similar to mutations for *Lfng(Serth et al., 2003)*. Thus, oscillatory expression, but not the expression itself, of the cyclic genes is important for coordinated somite segmentation. Hes7 acts as a transcriptional repressor and binds *Hes7* and *Lfng* promoter regions(Bessho et al., 2003). Hes7 forms a negative feedback loop by inhibition of its own promoter activity, and these mechanisms allows to periodic expression of *Hes7* and *Lfng* in the PSM (Fig. 3A)(Bessho et al., 2003). Moreover, Lfng also establishes a negative feedback loop, in which activation of Notch signaling induces *Lfng* expression, but Lfng protein inhibits Notch signaling and thereby represses the expression of *Lfng* (Fig. 3A)(Dale et al., 2003; Serth et al., 2003). Actually, not only the expression of Notch downstream genes oscillates, but also levels of Notch activity oscillate (Fig. 4A, B)(Morimoto et al., 2005). Now, it is thought that Notch signaling plays the central role in the segmentation clock determining temporal periodicity of somitogenesis.

The translation of the temporal information into the spatial periodicity of somites, is proposed to be mediated by the wavefront which regresses continually along AP axis of the PSM. Oscillating cells set their output when they encounter the regressing wavefront, leaving the segmental pattern of somites. Recent studies

suggested that FGF signaling is critical for this process. *Fgf8* transcripts are distributed along a caudorostral gradient in the posterior PSM, which is converted into graded FGF8 protein, which correlates with graded phosphorylation of the kinase Akt and MAPK, downstream effecters of FGF signalling(Delfini et al., 2005; Dubrulle and Pourquie, 2004b). The position of the wavefront has been proposed to be defined by a threshold activity of FGF signaling(Dubrulle et al., 2001; Sawada et al., 2001). However, the detailed molecular mechanisms involved in this process are not understood yet.

The basic helix-loop-helix (bHLH) gene *Mesp2* is a crucial factor in somitogenesis. *Mesp2* shows dynamic and periodical expression in the anterior PSM (expected wavefront), and segmentation border is not created in the Mesp2-null mouse (Fig. 5C)(Saga et al., 1997; Saga and Takeda, 2001; Takahashi et al., 2000). In previous study, Morimoto et al. generated a Mesp2-venus knock-in mouse in which Mesp2 protein localization in living embryo, and the anterior border of the expression domain of Mesp2 protein coincides with the next segmental border in the PSM (Fig. 5A,B), in which Mesp2 suppress Notch signaling, partly through the activation of *Lfng*, and allows boundaries formation of somite at the interface between Notch-activated and -repressed domains(Morimoto et al., 2005). It is thought that the temporal information provided by the segmentation clock appears to be translated by the expression and the function of Mesp2 in the anterior PSM.

To understand dynamic expression of *Mesp2*, Haraguchi et al. have mapped the enhancer activities required for the PSM within 185bp upstream region of 5'

flanking region of *Mesp2* gene (Fig. 5D)(Haraguchi et al., 2001), and Yasuhiko et al. have shown that T-box transcriptional factor, Tbx6, directly binds to enhancer elements, and is essential for the activation of *Mesp2(Yasuhiko et al., 2006)*. Furthermore, they demonstrate that Notch signaling strongly enhances *Mesp2* activation by Tbx6 (Fig. 5E)(Yasuhiko et al., 2006). However, the enhancer analysis was mainly based on the cultured cell system, the mechanism involved in the spatially restricted and the periodic regulation was remained to be elusive.

The purpose of this study is to reveal the mechanism, which enables the spatially restricted and periodic *Mesp2* expression in vivo situation, and reveal the mechanism required for the creation of the periodic pattern during somitogenesis.

RESULT

The temporal regulation of *Mesp2* transcription

Initially to investigate the link between the segmentation clock and the spatio-temporal regulation of *Mesp2* transcription, I employed high-resolution fluorescent in situ hybridization together with immunostaining to detect active Notch (Notch Intracellular Domain, NICD). The transcriptional state of *Mesp2* in each cell was thus visualized using intronic and exon mix probes (Fig. 6A) and could be divided into four distinct patterns (Fig. 6B); no transcription, initiation, active state and termination, allowing to trace the time course events of *Mesp2* transcription .I also defined a Notch standard time (phase-I, -II or -III) (Fig. 4B), which was dependent on the location of the Notch active domain in the posterior PSM and was used to monitor the segmentation clock. This double staining system enabled us to investigate the spatio-temporal regulation of different factors during somitogenesis.

During phase-II, when the oscillating Notch activity had not yet reached the anterior PSM, no *Mesp2* transcripts were detectable (Fig. 7A, B). However, once the Notch activity had reached the anterior PSM (Phase-III), *Mesp2* transcripts were evident in a portion of the cells within the relatively broad domain containing active Notch-positive cells (Fig. 7C, D). Most of these cells showed nuclear dots and some began to accumulate *Mesp2* transcripts in their cytoplasm (Fig. 7G, H). In phase-I, when the active-Notch domain had shrunk to a clear stripe in the anterior PSM and a new wave commenced from the posterior PSM, a stronger *Mesp2* signal was observed within the

active Notch domain (Fig. 7E, F). The signals at this point could now be observed in the cytoplasm in addition to nuclear dots in the majority of cells (Fig. 7I, J). It should be noted also that the cells exhibiting *Mesp2* transcription have a clear anterior limit and no *Mesp2* signal was detected beyond this border, even though the cells anterior to the border showed similar levels of active Notch. This indicated that Notch activity may decide the timing of *Mesp2* transcription but not the location. I speculated that Tbx6 would provide the spatial information required for *Mesp2* transcription.

Tbx6 defines the anterior border of Mesp2 expression

Using antibody against Tbx6, I performed whole mount immunohistochemistry and found that expression domain of Tbx6 protein has a clear anterior border (Fig. 9A, B). To investigate the link between the expression domain of Tbx6 protein and the spatio-temporal regulation of *Mesp2* transcription, I employed high-resolution fluorescent in situ hybridization together with immunostaining to detect Tbx6. I found that the Tbx6 border is perfectly matched with that of Mesp2 transcription (Fig. 8C-L), in either phase-III or -I, when *Mesp2* transcription is detectable. This result indicates that Tbx6 defines the anterior limit of Mesp2 expression domain by serving as an important transcription activator as we have shown before. However, the question that then arose was how this Tbx6 anterior domain is established. I subsequently found that the answer was provided by a double staining of Mesp2 and Tbx6 proteins.

Differing from the *Mesp2* transcript, the expression domain of Mesp2 protein was completely segregated from that of Tbx6 (Fig. 9A, B), indicating that once *Mesp2* is

activated by Tbx6 and translated to the protein it might suppress Tbx6 expression cell autonomously. This prediction was also supported by the analysis of Mesp2-null embryo in which Tbx6 protein expression was expanded to the anterior somitic region (Fig. 9C, D). Intriguingly, the *Tbx6* transcript detected by in situ hybridization was not extended even in the Mesp2-null embryo and it was almost similar to that in the wild-type control embryo (Fig. 9E, F). The result indicates that Mesp2 is involved in the posttranslational regulation of Tbx6 protein and in the absence of Mesp2, Tbx6 protein is stabilized and stayed longer time, at least 12 hours by my estimation (Fig. 9G). The stabilized Tbx6 proteins would then be responsible for the Mesp2-null mouse phenotype, in which both *Dll1* expression and *Mesp2* transcription is expanded (previously revealed by our analysis of a *Mesp2-LacZ* knockin embryo)(Takahashi et al., 2000), as *Dll1* transcription has been shown to be activated by Tbx6(Galceran et al., 2004; Hofmann et al., 2004; White and Chapman, 2005).

Periodic somite formation is made possible by negative regulations of Notch activity and Tbx6 expression by Mesp2

My results indicate that interactions of three factors, Mesp2, Tbx6 and Notch activity are critically important to translate temporal information to the spatial patterning. To define the dynamic regulatory network, I decided to investigate in detail spatio-temporal relationships between three factors during somitogenesis. To achieve this, totally 20 embryos were prepared at E10.5 and three sections from each embryo were subjected to double immunostainings for Mesp2 and NICD, Mesp2 and Tbx6, and

NICD and Tbx6, respectively, which enable me to determine their relationship in a fixed time point. According to the Notch standard time in Figure 4B, I rearranged these results and the temporal and spatial dynamics of these expressions was resolved. There are distinct patterns depending on segmentation stages. First in the Phase-III, once Notch activity reached in the anterior PSM, in which *Mesp2* transcription had been initiated, Mesp2 protein started to be detected in the posterior part of NICD domain just like *Mesp2* transcripts (Fig. 10B). This region also corresponds to the anterior limit of Tbx6 expressing domain (Fig. 10C). In the phase-I, at 30-40 minutes later, Mesp2 expression domain overlapped with those of NICD and Tbx6 (Fig. 10E), in which Tbx6 expression started to be repressed by Mesp2 (Fig. 10F). In the phase-II, when the second wave just reached the anterior PSM region, three signals showed complete segregation, which resulted in a boundary formation between NICD and Mesp2 (Fig. 10H), thus demarcating the next segmental border as previously described, which demarcates the next segmental border through the activation of Lfng by Mesp2(Morimoto et al., 2005), and a boundary between Mesp2 and Tbx6 (Fig. 10I), which will be the next Mesp2 anterior limit and thus the second segmental border.

The next question is when and how the cycle of these three factors established. To address this question, I focused on the early stage embryos that had no segmented somite from E6.5 to E7.5, and one showing first segmented somite at E8.0. I have noticed two distinct patterns in the Tbx6 expression. One showed graded expression without clear anterior limit, which were observed at E6.5 to E7.0 (Fig. 11E, F), the other showed the expression with clear anterior limit and found at E7.5 to E8.0 (Fig. 11G, H).

These patterns were closely linked to the absence (Fig. 11A, B) or presence (Fig. 11C, D) of Mesp2 protein. Further immunohistological analysis using sections revealed that no clear Notch signal oscillation is started yet in the nascent mesodermal layer in the early stage embryos without Mesp2 expression although both NICD and Tbx6 expression were detected (Fig. 12A-C). In the slightly later stage embryos that are characterized by the clear anterior boundary of Tbx6 protein and the presence of Mesp2 expression stripe (Fig. 12E, F), oscillatory pattern of Notch activity was detected and the spatial patterns of three factors were similar to those of later stage embryos (Fig. 12G, H), indicating that the spatio-temporal relationship has been established in this stage embryos. The clear difference between there two groups of embryos was absence or presence of Notch signal oscillation, indicating that the initiation of Notch signal oscillation triggers the first Mesp2 expression.

Posterior border of Mesp2 expression is defined by FGF and Wnt signal

A remaining question of the spatio-temporal regulation of *Mesp2* transcription to be answered is the mechanism to define the posterior border of Mesp2 expression. In other word, what would determine the width of single somite and why Mesp2 expression is suppressed in the posterior PSM. It is suggested that Mesp2 expression domain is defined by so-called the wavefront, which is proposed to be defined by gradient FGF signaling in the chick system(Delfini et al., 2005).

I examined the expression pattern of *Dusp4*, an FGF signaling target gene that shows an oscillation pattern in the posterior PSM(Niwa et al., 2007). Interestingly, the

anterior limit of the *Dusp4* expression domain was found to accord with the posterior limit of *Mesp2* (Fig. 13A-D), which supported the possibility that FGF signaling determined the posterior border of *Mesp2* expression domain by negatively regulating *Mesp2* expression. The *Dusp4* expression pattern was unchanged and was not anteriorly expanded in the absence of Mesp2 (Fig. 13E-F), which was different from that of Tbx6 protein, a positive regulator of *Mesp2* expression .

Next, I examined whether the *Mesp2* expression domain was altered by the lack of FGF signaling. Because somites are not formed in FGFr1 (FGF receptor1) null mice due to misspecification of paraxial mesoderm(Itoh et al., 1996), it is not possible to examine these mice for the *Mesp2* expression. In recent study, The PSM-specific FGFr1 knockout mice was generated by crossing floxed FGFr1 mutant mice and Hes7-cre mice, and I used these mice(Niwa et al., 2007; Xu et al., 2002). The PSM-specific FGFr1 knockout (Fgfr1-cKO) results in a gradual loss of PSM supply and the truncation of the tailbud(Niwa et al., 2007; Wahl et al., 2007). As expected, a posterior shift in the *Mesp2* expression domain was consistently observed in all of the specimens (Fig. 14A). However, *Mesp2* expression was not completely regressed to the posterior end of the PSM, indicating the presence of other factors responsible for positioning the determination wavefront. The lower levels of *Mesp2* expression may account for the anterior expansion of the Tbx6 expression domain (Fig. 14B). Using the specimens which showed less truncation of the PSM, I examined the relationship among Mesp2, Notch and Tbx6 by immunohistochemistry. Tbx6 expression was observed in the PSM without a clear anterior border, and this was accompanied by the anterior expansion of

Mesp2 expression in the Fgfr1-cKO embryo (Fig. 14C, D). Lower but continuous Notch activity was observed in the posterior PSM without apparent oscillation in the Fgfr1-null embryo, as shown earlier, and a higher level of Notch activity almost merged with that of the Mesp2 expression domain, suggesting that the posterior shift of active Notch domain caused by the lack of FGF signaling is responsible for the posterior shift of Mesp2 (Fig. 14E, F).

Another possible factor involved in the positioning of the *Mesp2* expression domain is Wnt signal, since it was recently shown that the ectopic activation of b-catenin in the PSM leads to the anterior shift of the wavefront(Aulehla et al., 2007; Dunty et al., 2008). I examined the expression of *Mesogenin1(Msgn1),* one of the downstream targets of Wnt signaling(Wittler et al., 2007). In the wild-type embryo, *Msgn1* was expressed in the posterior PSM but declined posterior to the anterior limit of *Dusp4* domain, thereby forming a gap between *Mesp2* and *Msgn1* expression domains (Fig. 15A-D). Like *Dusp4,* the expression pattern of *Msgn1* was unchanged in the Mesp2-null embryo (Fig. 15E, F). Thus, Wnt signaling also works upstream of Mesp2 but is unlikely to determine the posterior limit of *Mesp2* expression domain. Nevertheless it could be involved in the suppression of *Mesp2* in the posterior PSM since Wnt signaling is known to be maintained in the absence of FGF signaling.

My results are schematically summarized in Figure 19. I propose that the periodic activation of *Mesp2* in the anterior PSM is achieved by the cooperative function of two positive factors, Tbx6 (spatial factor) and Notch (temporal factor), and by negative factors provided from the posterior end by pathways such as FGF and Wnt signaling.

T-box dependent suppression of Tbx6 protein

The most intriguing finding in my current study is the suppression of Tbx6 by Mesp2. The next question to be answered is the mechanism by which Mesp2 suppresses Tbx6 expression post-translationally. Because Tbx6 protein expression was stabilized and expanded to the anterior region in Mesp2-null embryo, it is expected that Tbx6 proteins were degraded at the downstream of Mesp2. To reveal the mechanism of Tbx6 suppresion, I used BAC (Bacterial artificial chromosome)-based technology for the identifcation of the domain, which is essential for the degradation of Tbx6 protein. BAC modification technology is a powerful method for the exogenous genes, expressing at the specific expression. I used the λ recombinase mediated homologous recombination system, which is easy to modify the BAC clone, because a DNA fragment required for the homologous recombination is simply generated by PCR amplification (Fig. 16A)(Datsenko and Wanner, 2000). I tried to express the several types of Tbx6 protein, which have truncation in several domains under the control of endogenous promoter and enhancers of *Tbx6*. I have obtained a BAC clone (PR24-66B9) spanning 202 kb, which contains totally 5 genes including *Tbx6* (Fig. 16B). Whether this BAC clone reproduce the endogenous expression of *Tbx6*, I introduced Venus-tag before the *Tbx6* stop codon site and created BAC-Tbx6-Venus construct (Fig. 16C). BAC-Tbx6-Venus expresses full length Tbx6 fused with venus. Using BAC-Tbx6-Venus, I confirmed the expression pattern of Venus protein by transient transgenic

analyses, can found that expression domain of Tbx6-Venus protein has a clear anterior border similar to the enodonogenus Tbx6 protein (Fig. 17B). Next, I introduced Venus-tag into the translational initiation site of *Tbx6* and created BAC-Venus (Fig. 16C), which expresses only Venus. I confirmed that expression of Venus protein was expanded to the anterior region (Fig. 17A), because Venus protein is more stable. From these results, it was proud that BAC-based technology is a good system to distinguish the amino acid sequences include or exclude the degradation domain. Next, I created BAC-Tbx6 Δ C-Venus, which expresses Tbx6 which has no C terminal region fused with Venus (Fig. 16C), and BAC-Tbx6 Δ CT-Venus, which expresses only N terminal region of Tbx6 fused with Venus (Fig. 16C). Tbx6 Δ C-Venus protein has a clear anterior border (Fig. 17C), however Tbx6 Δ CT-Venus protein was expanded to the anterior region (Fig. 17D). These results indicated that T-box, DNA-binding motif of Tbx6, is essential for the degradation of Tbx6 protein downstream of Mesp2.Next, I created BAC-Tbox-Venus (Fig. 16C), which expresses only T-box region of Tbx6 fused with Venus. Interestingly, Tbox-Venus protein has a clear anterior border, indicating that DNA-binding motif of Tbx6 is sufficient of the degradation (Fig. 17E).

Mesp2 also suppresses Brachyury protein at the posttranslational mechanism

To examine that the T-box dependent degradation is general mechanism for T-box transcriptional factor, I tried to perform immunostaining for other T-box factor protein, Brachyury. *Brachyury* mRNA only exists at the tail bud region (Fig. 18A), not similar to the *Tbx6* transcript (Fig. 18B), but Brachyury protein exists at the anterior PSM region

(Fig. 18C). Interestingly, I can found that expression domain of Brachyury protein has a clear anterior border (Fig. 18C), and Brachyury protein expression was expanded to the anterior somitic region in the Mesp2-null mouse (Fig. 18D). I also performed the double immunostainings for Tbx6 and Brachyury, the anterior border of these protein were perfectly matched (Fig. 18E-G), indicating that Brachyury protein was suppressed at the same post translational mechanism by Mesp2.

Discussion

Mesp2 is an output signal of the segmentation clock

The periodicity of mouse somitogenesis has been explained by the nature of segmentation clock centered by the function of Notch signaling, in which Notch signal activates Hes7, which represses own transcription and that of L-fng, which act as a negative regulator of Notch activity(Bessho et al., 2003; Bessho et al., 2001; Morimoto et al., 2005). These mechanisms allow to the oscillation of Notch signal activity within the PSM(Horikawa et al., 2006; Huppert et al., 2005; Morimoto et al., 2005). These oscillations in individual cells are known to be synchronized by cellular interaction via Notch signaling, which serves as a coupled oscillator within the PSM(Horikawa et al., 2006; Jiang et al., 2000; Mara et al., 2007). However, the oscillation itself does not make a segmental boundary, as exemplified by a pendulum clock in which indication of the correct time is not provided by the rhythm of pendulum. The periodic information has to be read as an output of the clockwork linked with the oscillation. In the current study, I focused on the molecular mechanism how the segmentation clock is correctly translated to the segmental information. I found the temporal link between Notch signal oscillation and Mesp2 transcription cycle. In addition, I found that the transcription was made possible only in the cells having Tbx6 expression without FGF signaling (Fig. 19). Hence, the rhythm (periodicity) is generated by segmentation clock in the posterior PSM and segments are generated according to the information. Hence, I propose that the final output of the clockwork is the induction of Mesp2 transcription factor.

Establishment of the periodic pattern of the somitogenesis

The metameric structures in vertebrates are based on the periodicity of somites formed one by one from the anterior part of PSM. The transcriptional on/off of *Mesp2* is also repeated in the anterior part of PSM, which leads to generating the periodicity of somites. In this study, I found the mechanism how the periodic *Mesp2* transcription is achieved in the anterior PSM. *Mesp2* is activated by Tbx6-dependent Notch activity but in turn Mesp2 strongly suppresses Tbx6 expression as well as Notch activity. The negative regulation of the Tbx6 by Mesp2 is critically important to set up the next anterior border of *Mesp2* expression domain which also marks a next segmental border. Therefore, the reciprocal regulation between Mesp2 and Tbx6 is the heart of the mechanism to create periodic patterning during somitogenesis. I also found that onset of *Mesp2* transcription is closed linked with the initiation of Notch signal oscillation, indicating that onset of the Notch signal oscillation trigger the reciprocal regulation between Mesp2 and Tbx6, and initiate the sequential creation of somites in a head-to-tail fashion. The next critical question would be the mechanism by which Notch signal oscillation initiate during embryogenesis. Importantly, *Hes7* and *Lfng*, that are essential for segmentation clock, were also expressed but not oscillated in earlier stage embryos (E.7.0, date not shown), when no clear Notch signal oscillation existed regardless of presence of both NICD and Tbx6 expression. I speculate that only presence of negative regulators signals, *Hes7* and *Lfng* is not enough to create cyclic patterns of gene

expression, but the precise expression level and the precise regulations must be required to initiate somitogenesis.

Establishment of rostro-caudal (RC) polarity by the suppression of Tbx6

After somites separate from the PSM, somite cells begin to differentiate into axial structures in response to signals derived from the surrounding tissues. The sclerotome of each somite is subdivided into rostral and caudal compartments, and each compartment then re-fuses with its neighbor to form a vertebra. This 'resegmentation' process recreates segment borders within the sclerotome to generate parts of two neighboring vertebrae; the division reflects the pre-existing rostrocaudal polarity of the somite. The rostral compartment of the somite gives rise to caudal half of vertebral body and intervertebral disc, whereas the caudal compartment generates the rostral half of the vertebral body and the pedicle of the neural arch(Tam et al., 2000). The rostro-caudal polarity of each somite is established within the PSM before segmentation. Expressions of *Dll1,* which is ligand of Notch signal, are subdivided into two regions, region-1 is expression of posterior PSM, and region-2 is expressions of anterior PSM and somite(Takahashi et al., 2000). Previously it has been shown that the level and pattern of *Dll1* expression in region-2 prefigure the segmental features of vertebrae (Fig. 20A, C)(Takahashi et al., 2000). *Dll1* expression in region-2 in wild-type embryos is restricted to the caudal half of somite primordia, and the caudal expression is maintained after somite borders have formed (Fig. 20A). In the embryos of *Mesp2* knockout mice, in which *Dll1* expression in region-2 is expanded, vertebrae are

caudalized (Fig. 20D, F)(Takahashi et al., 2000). By contrast, in the null embryos of *PS1*, which encodes a *presenilin 1* that is essentially for processing and activation of Notch, which show no caudal expression of *Dll1* in region-2 but maintain normal *Dll1* expression in region-1, the vertebrae are rostralized (Fig, 20G, I)(Takahashi et al., 2000). Therefore, *Dll1* expression of PSM are regulated by two independent pathways, One is the *Dll1* expression in region-1 which is independent on the Notch signal, the other is the caudal *Dll1* stripe in region-2 which is dependent on the *PS1* mediated Notch signal, and Mesp2 establishes rostro-caudal (RC) polarity by suppressing the *Dll1* expression in region-2(Takahashi et al., 2000). But, in previous studies, the real target of Mesp2 function had not been understood. In this study, I found that Tbx6 is a real target of Mesp2 function, since *Dll1* in region-1 is a downstream target of Tbx6(Galceran et al., 2004; Hofmann et al., 2004; White and Chapman, 2005). In the absence of Mesp2, Tbx6 is expanded anteriorly, which accounts for the anterior expansion of *Dll1* in region-2, and it leads to somite caudalization (Fig. 20D-F). In the absence of *PS1*, Tbx6 is normally expressed and thus it maintains normal *Dll1* expression in region1. However, there is no caudal expression of *Dll1* in region-2 since PS1-dependent Notch signaling is absent, and it leads to somite rostrolization (Fig. 20G-I). In addition, my model also explains how the RC polarity is established during normal somitogenesis. The process is clearly shown in Fig. 21: During phase I-II, Mesp2 suppresses *Dll1* expression within the one somite length via suppressing Tbx6 (Fig. 21A, C) .In the phase-III, the next Notch wave comes on in the region, which includes the presumptive caudal compartment of somite that has already experienced Mesp2 expression and the next

presumptive somite. Finally, the caudal *Dll1* stripe is generated by Notch activation dependent of PS1 (Fig. 21F).

Post-translational suppression of Tbx6 protein allow to rapid change of Tbx6 activity

The intervals of each somite formation are strictly defined for each species (30 minutes in zebrafish, 90 minutes in chick, 2 hours in mouse). It is demonstrated that the rapid change of the protein level is very important for somitogenesis. In fact, Hes7 protein is unstable because of the rapid degradation by the ubiquitin-poteasome system, in which half-life of Hes7 protein is approximately 20 min(Bessho et al., 2003). Mice with Lysine 14 to Arginine mutation in the Hes7 locus, which makes the half-life of Hes7 protein approximately 30 min without changing the transcriptional repressor activity, display damped oscillation after several cycles, indicating that rapid change of Hes7 protein activity is essential for the correct somitogenesis(Hirata et al., 2004). In the current study, I find that the negative regulation of Tbx6 is posttranslational level, and the rapid change of the Tbx6 protein activity is important for creating the periodicity of somitogenesis. I think that Tbx6 protein is degraded at the downstream of Mesp2, however the mechanism by which Mesp2 suppresses Tbx6 expression post-translationally is currently unknown. The identification of the direct targets of Mesp2 and further clarification of the genetic network in which this transcription factor exerts its functional role will be required to resolve this complex and sophisticated segmentation program.

T box-dependent degradation of Tbx6/ Brachyury protein

There are several examples showing that the activity of transcription factors is regulated by a protein degradation system. These transcription factors have the domain required for the protein degradation, which generally exists outside of the DNA-binding motif, and have their own protein degradation mechanisms. However, both Tbx6 and Brachyury have such domains within the DNA-binding domain. From these results, I speculate that other T-box transcriptional factors might also be regulated by the similar degradation mechanism, which is depending on DNA-binding domain, T-box. Since T-box transcriptional factors are implicated in many developmental events during embryogenesis, I also speculate that T-box protein might be involved in the switch mechanisms of gene activity required for the quick response upon some signaling cascades. Next crucial question would be determining the amino acid sequence that is essential for the degradation of Tbx6 protein, to ask whether these sequences are separated from that of the DNA-binding motif in the T-box. It would be important to know whether these sequences are conserved within the T-box families and also conserved evolutionarily among species. The change of transcriptional state from activation to inactivation and vice versa would be critically important for developmental events. This switch should be rapid in particular situation, because many developmental events need quick changes, therefore protein degradation of transcriptional factors provide a simple and useful mechanism to allows a rapid change of gene activity from activation to inactivation state. Hence, I hope a finding of the mechanism involved in

the T-box protein degradation during somitogenesis would lead to the understanding of transcriptional regulation in other developmental processes.

Material and Methods

Animals

The wild-type mice used in this study are MCH (a closed colony established in Clea, Japan). The Mesp2-null mouse (Mesp2-LacZ knock in mouse) was maintained in the animal facility in National Institute of Genetics, Japan. The conditional Fgfr1 knockout mouse was generated by crossing an Fgfr1 floxed mouse with a Hes7-cre mouse and the embryos were recovered at E9.5-10.5. Noon on the day of the copulation plug was defined as embryonic day (E) 0.5.

Whole mount in situ hybridization and immunohistochemistry

The InsituPro system (M&S Instruments) was used for whole mount in situ hybridization according to the manufacturer's instructions. Whole mount immunohistochemistry was performed using an anti-Tbx6 and anti-Mesp2 antibody described previously.

Section in situ hybridization and immunohistochemistry.

Mouse embryo and tail samples were fixed in 4% PFA, embedded in OCT compound and frozen in liquid nitrogen. For double in situ hybridizations, frozen sections (8 μ m) were hybridized with digoxigenin-labeled antisense cRNA probes (Roche) for *Dusp4* and biotin-labeled antisense cRNA probes (Roche) for *Mesp2*. Hybridized DIG-probes were detected using a horseradish peroxidase-conjugated anti-DIG sheep antibody (Roche) and Cyanin3 Tyramid (Perkin Elmer) signal detection. Hybridized Biotin-

probes were detected using horseradish peroxidase conjugated Streptavidin (Roche) and fluorescein isothiocyanate conjugated Tyramid (Perkin Elmer) signal detection. For double immunohistochemistry, frozen sections (8μm) were immersed in unmasking solution (Vector Laboratories) and autoclaved at 105°C for 15 min to enable antigen retrieval. Antibody reactions and the detection of Notch1 activity, Mesp2 and Tbx6 were separately conducted after antigen retrieval. The detection of Notch1 activity or Mesp2 was performed by incubation with anti-active-NICD (1:200, Cell Signaling Technology) or anti-Mesp2 (1:400) primary antibodies, respectively, followed by incubation with horseradish peroxidase-conjugated anti-rabbit IgG donkey antibody (1:200, Amersham Pharmacia Biotech) and treatment with Cyanin3-Tyramid (Perkin Elmer). For the detection of Mesp2 or Tbx6, anti-Mesp2 (1:400) or anti-Tbx6 (1:1000), horseradish peroxidase-conjugated anti-rabbit IgG donkey antibodies (1:400, Amersham Pharmacia Biotech) were used, respectively, followed by fluorescein isothiocyanate conjugated Tyramid (Perkin Elmer) signal detection.

For double staining using immunohistochemistry and in situ hybridizations, frozen sections (8μm) were immersed in unmasking solution (Vector Laboratories) and autoclaved at 105°C for 15 min to enable antigen retrieval. Notch1 activity and Tbx6 were detected by incubation with anti-active-NICD (1:200, Cell Signaling Technology) or anti-Tbx6 (1:1000) primary antibodies, followed by a biotinylated goat anti-rabbit IgG secondary antibody (1:200, Vector Laboratories). These sections were then hybridized with digoxigenin labeled antisense cRNA probes (Roche). The hybridized probes were detected using horseradish peroxidase-conjugated anti-DIG sheep

antibodies (Roche) and Cyanin3-Tyramid (Perkin Elmer) signal detection. Notch1 activity and Tbx6 were detected using horseradish peroxidase-conjugated Streptavidin (Roche) and fluorescein isothiocyanate conjugated Tyramid (Perkin Elmer) signal detection.

For detection of Venus, sections were prepared for frozen sections (8μm).Venus protein were detected by incubation with anti-GFP (1:200, MBL) primary antibodies, followed by a Alexa 488 goat anti-rabbit IgG secondary antibody (1:200, Molecular Probes).

Each section was occasionally counterstained with 0.5 μg/ml of 4'-6-diamino-2-phenylin-dole (DAPI) for 10 min and examined using an Olympus BX61 fluorescence microscope system with an ORCA-ER digital camera (HAMAMATSU photo). Subsequent analysis was undertaken using MetaMorph software (Universal Imaging).

BAC modification system

BAC DNA modifications were generated using the λ red recombination method as described previously by(Datsenko and Wanner, 2000). Briefly, we used 70 nt primers with 50 nt of homology to the gene of interest at the 5_ end and 20 nt of homology to the FRT-flanked kanamycin resistance cassettes at the 3_ end (Fig. 18A). The resulting PCR products were concentrated using Qiagen PCR purification columns. We generated electroporation-competent DH10 BAC host cells and then transformed them with PKD46 which carries the λ recombination genes *gam, bet*, and *exo* under the control of the *araBAD* promoter (Datsenko and Wanner, 2000), Colonies hosting both BAC and pKD46 were grown overnight at 30°C and diluted 1/100 in LB Amp/0.1 M L-

arabinose and grown to an OD_{600} of 0.6. Electrocompetent cells were prepared and transformed with approximately 500 ng of PCR product and recovered in 1 ml of SOC for 2 h and plated onto LB plates containing chloramphenicol and kanamycin at 37°C. The resulting colonies were then characterized using specific PCR. The primers used in this study are shown below.

Generation of BAC-Tbx6-Venus

(For modifications of BAC, Forward primer: BAC-Venus-F)

TTAGACCCCGGATTCTAGCAACGGGACACAAGGCCAGAAGAAACTACAACA

TGGTGAGCAAGGGCGAGGA

(For modifications of BAC, Reverse primer: BAC-Venus-R)

AGACGGTAGCCAGTCCCCAGGGAGGGGTACAACTCTCGTGGATGGTACATGT

GTAGGCTGGAGCTGCTTC

(For recombination check of BAC, Forward primer: BAC-Venus-F2)

TTGGAAGGGGCTGTGCTGTGAGCT

(For recombination check of BAC, Reverse primer: BAC-Venus-R2)

GGTGGGAAGGTGGAGTCTGCCCCA

Generation of BAC-Tbx6-Venus

(For modifications of BAC, Forward primer: BAC-Tbx6-Venus-F)

TACCGTACCCAGGACCTGGAGGTTATCTGGACATGGGATCCAAGCCAATGAT

GGTGAGCAAGGGCGAGGA

(For modifications of BAC, Reverse primer: BAC-Tbx6-Venus-R)

TACCGTACCCAGGACCTGGAGGTTATCTGGACATGGGATCCAAGCCAATGAT

GGTGAGCAAGGGCGAGGA

(For recombination check of BAC, Forward primer: BAC-Tbx6-Venus-F2)

TTCATCCAAGGGGGTCCCTTCC

(For recombination check of BAC, Reverse primer: BAC-Tbx6-Venus-R2)

AGGGGGATACCACTTCAATGCGG

Generation of BAC-Tbx6 Δ TC-Venus

(For modifications of BAC, Forward primer: BAC-Tbx6 Δ TC-Venus-F)

TGGGCCCCGAGACAGCACCGCCACCCCCAGAGGCCCTTCACTCGCTTCCTGT

GAGCAAGGGCGAGGAGCT

(For modifications of BAC, Reverse primer: BAC-Tbx6 Δ TC-Venus-R)

GCGCTGAATTCCTTCCACAGTTCCTGGTTCTCCAAGCTCAGGCTGACCCCGT

GTAGGCTGGAGCTGCTTC

(For recombination check of BAC, Forward primer: BAC-Tbx6 Δ TC-Venus-F2)

GGATCGAGGCAGCTCCCCACACTC

(For recombination check of BAC, Reverse primer: BAC-Tbx6 Δ TC-Venus-R2)

ACCTGCCAGCCTTGGTGATGATC

Generation of BAC-Tbx6 Δ TC-Venus

(For modifications of BAC, Forward primer: BAC-Tbx6 Δ C-Venus-F)

CACCACCATCATTCCCCAGGGAGCGGGATGCCCGTGTGAAGAGGAAACTTGT

GAGCAAGGGCGAGGAGCT

(For modifications of BAC, Reverse primer: BAC-Tbx6 Δ C-Venus-R)

CTCACCCCCACTCCCACAGGCCTCTGTGGCCACTGGCTCTGGGCCCCGGTGT

AGGCTGGAGCTGCTTC

(For recombination check of BAC, Forward primer: BAC-Tbx6 Δ C-Venus-F2)

AGTACTATTAGTGCCATCATCATC

(For recombination check of BAC, Reverse primer: BAC-Tbx6 Δ C-Venus-R2)

GGGGAGGTTCCATGTCTCAGTTTT

Generation of BAC-Tbox-Venus and Generation of BAC-TboxN-Venus

(For modifications of BAC, Forward primer: BAC-Tbox-Venus-F)

TTAGACCCCGGATTCTAGCAACGGGACACAAGGCCAGAAGAAACTACAACA

TGGTGGGGGTCAGCCTGAGCTTGG

(For modifications of BAC, Reverse primer: BAC-Tbox-Venus-R)

AGACGGTAGCCAGTCCCCAGGGAGGGGTACAACTCTCGTGGATGGTACATGT

GTAGGCTGGAGCTGCTTC

(For recombination check of BAC, Forward primer: BAC-Tbox-Venus-F2)

TTCATCCAAGGGGGTCCCTTCC

(For recombination check of BAC, Reverse primer: BAC-Tbox-Venus-R2)

AGGGGGATACCACTTCAATGCGG

Generation of transgenic mice

All constructs were digested with restriction enzymes to remove vector sequences and then gel purified. Transgenic mice were generated by microinjection of fertilized eggs. Microinjected eggs were then transferred into the oviducts of pseudopregnant foster

females. We sacrificed the foster mouse to recover embryos at E10.5. The genotypes of the embryos were identified by PCR using yolk sac DNA.

Acknowledgements

I thank Drs. Yumiko Saga and Hiroki Kokubo for supervising my entire research; I thank member of Mammalian Development Laboratory for valuable suggestion and support; the members of Progress Report Committee, Drs. Toshihiko Shiroishi, Susumu Hirose, Yasushi Hiromi, Takako Isshiki, Kenta Sumiyama, Takashi Sado for critical advice and discussion; Dr. Chu-Xia Deng for providing floxed Fgfr1; Dr. Yasutaka Niwa for produced the Fgfr1-conditional knockout mouse and prepared embryos; Dr Deborah L. Chapman for providing Tbx6 antibody; Dr. Barry L. Wanner for providing us with pKD46; Drs. Tatsumi Hirata and Toshiyuki Hatano for technical support of BAC modification.

Reference

Aulehla, A., Wiegraebe, W., Baubet, V., Wahl, M. B., Deng, C., Taketo, M., Lewandoski, M. and Pourquie, O. (2007). A beta-catenin gradient links the clock and wavefront systems in mouse embryo segmentation. *Nat Cell Biol.*

Bessho, Y., Hirata, H., Masamizu, Y. and Kageyama, R. (2003). Periodic repression by the bHLH factor Hes7 is an essential mechanism for the somite segmentation clock. *Genes Dev* 17, 1451-6.

Bessho, Y., Sakata, R., Komatsu, S., Shiota, K., Yamada, S. and Kageyama, R. (2001). Dynamic expression and essential functions of Hes7 in somite segmentation. *Genes Dev* 15, 2642-7.

Cooke, J. and Zeeman, E. C. (1976). A clock and wavefront model for control of the number of repeated structures during animal morphogenesis. *J Theor Biol* 58, 455-76.

Dale, J. K., Maroto, M., Dequeant, M. L., Malapert, P., McGrew, M. and Pourquie, O. (2003). Periodic notch inhibition by lunatic fringe underlies the chick segmentation clock. *Nature* 421, 275-8.

Datsenko, K. A. and Wanner, B. L. (2000). One-step inactivation of chromosomal genes in Escherichia coli K-12 using PCR products. *Proc Natl Acad Sci U S A* 97, 6640-5.

Delfini, M. C., Dubrulle, J., Malapert, P., Chal, J. and Pourquie, O. (2005). Control of the segmentation process by graded MAPK/ERK activation in the chick embryo. *Proc Natl Acad Sci U S A* 102, 11343-8.

Dubrulle, J., McGrew, M. J. and Pourquie, O. (2001). FGF signaling controls somite

boundary position and regulates segmentation clock control of spatiotemporal Hox gene activation. *Cell* 106, 219-32.

Dubrulle, J. and Pourquie, O. (2002). From head to tail: links between the segmentation clock and antero-posterior patterning of the embryo. *Curr Opin Genet Dev* 12, 519-23.

Dubrulle, J. and Pourquie, O. (2004a). Coupling segmentation to axis formation. *Development* 131, 5783-93.

Dubrulle, J. and Pourquie, O. (2004b). fgf8 mRNA decay establishes a gradient that couples axial elongation to patterning in the vertebrate embryo. *Nature* 427, 419-22.

Dunty, W. C., Jr., Biris, K. K., Chalamalasetty, R. B., Taketo, M. M., Lewandoski, M. and Yamaguchi, T. P. (2008). Wnt3a/ -catenin signaling controls posterior body development by coordinating mesoderm formation and segmentation. *Development* 135, 85-94.

Evrard, Y. A., Lun, Y., Aulehla, A., Gan, L. and Johnson, R. L. (1998). lunatic fringe is an essential mediator of somite segmentation and patterning. *Nature* 394, 377-81.

Galceran, J., Sustmann, C., Hsu, S. C., Folberth, S. and Grosschedl, R. (2004). LEF1-mediated regulation of Delta-like1 links Wnt and Notch signaling in somitogenesis. *Genes Dev* 18, 2718-23.

Haraguchi, S., Kitajima, S., Takagi, A., Takeda, H., Inoue, T. and Saga, Y. (2001). Transcriptional regulation of Mesp1 and Mesp2 genes: differential usage of enhancers during development. *Mech Dev* 108, 59-69.

Hirata, H., Bessho, Y., Kokubu, H., Masamizu, Y., Yamada, S., Lewis, J. and Kageyama, R. (2004). Instability of Hes7 protein is crucial for the somite segmentation clock. *Nat*

Genet 36, 750-4.

Hofmann, M., Schuster-Gossler, K., Watabe-Rudolph, M., Aulehla, A., Herrmann, B. G. and Gossler, A. (2004). WNT signaling, in synergy with T/TBX6, controls Notch signaling by regulating Dll1 expression in the presomitic mesoderm of mouse embryos. *Genes Dev* 18, 2712-7.

Horikawa, K., Ishimatsu, K., Yoshimoto, E., Kondo, S. and Takeda, H. (2006). Noise-resistant and synchronized oscillation of the segmentation clock. *Nature* 441, 719-23.

Huppert, S. S., Ilagan, M. X., De Strooper, B. and Kopan, R. (2005). Analysis of Notch function in presomitic mesoderm suggests a gamma-secretase-independent role for presenilins in somite differentiation. *Dev Cell* 8, 677-88.

Itoh, N., Mima, T. and Mikawa, T. (1996). Loss of fibroblast growth factor receptors is necessary for terminal differentiation of embryonic limb muscle. *Development* 122, 291-300.

Jiang, Y. J., Aerne, B. L., Smithers, L., Haddon, C., Ish-Horowicz, D. and Lewis, J. (2000). Notch signalling and the synchronization of the somite segmentation clock. *Nature* 408, 475-9.

Mara, A., Schroeder, J., Chalouni, C. and Holley, S. A. (2007). Priming, initiation and synchronization of the segmentation clock by deltaD and deltaC. *Nat Cell Biol* 9, 523-30.

McGrew, M. J., Dale, J. K., Fraboulet, S. and Pourquie, O. (1998). The lunatic fringe gene is a target of the molecular clock linked to somite segmentation in avian embryos. *Curr Biol* 8, 979-82.

Morimoto, M., Takahashi, Y., Endo, M. and Saga, Y. (2005). The Mesp2 transcription factor establishes segmental borders by suppressing Notch activity. *Nature* 435, 354-9.

Niwa, Y., Masamizu, Y., Liu, T., Nakayama, R., Deng, C. X. and Kageyama, R. (2007). The initiation and propagation of Hes7 oscillation are cooperatively regulated by Fgf and notch signaling in the somite segmentation clock. *Dev Cell* 13, 298-304.

Palmeirim, I., Henrique, D., Ish-Horowicz, D. and Pourquie, O. (1997). Avian hairy gene expression identifies a molecular clock linked to vertebrate segmentation and somitogenesis. *Cell* 91, 639-48.

Pourquie, O. (2003). The segmentation clock: converting embryonic time into spatial pattern. *Science* 301, 328-30.

Saga, Y., Hata, N., Koseki, H. and Taketo, M. M. (1997). Mesp2: a novel mouse gene expressed in the presegmented mesoderm and essential for segmentation initiation. *Genes Dev* 11, 1827-39.

Saga, Y. and Takeda, H. (2001). The making of the somite: molecular events in vertebrate segmentation. *Nat Rev Genet* 2, 835-45.

Sawada, A., Shinya, M., Jiang, Y. J., Kawakami, A., Kuroiwa, A. and Takeda, H. (2001). Fgf/MAPK signalling is a crucial positional cue in somite boundary formation. *Development* 128, 4873-80.

Serth, K., Schuster-Gossler, K., Cordes, R. and Gossler, A. (2003). Transcriptional oscillation of lunatic fringe is essential for somitogenesis. *Genes Dev* 17, 912-25.

Takahashi, Y., Koizumi, K., Takagi, A., Kitajima, S., Inoue, T., Koseki, H. and Saga, Y. (2000). Mesp2 initiates somite segmentation through the Notch signalling pathway. *Nat*

Genet 25, 390-6.

Tam, P. P., Goldman, D., Camus, A. and Schoenwolf, G. C. (2000). Early events of somitogenesis in higher vertebrates: allocation of precursor cells during gastrulation and the organization of a meristic pattern in the paraxial mesoderm. *Curr Top Dev Biol* 47, 1-32.

Wahl, M. B., Deng, C., Lewandoski, M. and Pourquie, O. (2007). FGF signaling acts upstream of the NOTCH and WNT signaling pathways to control segmentation clock oscillations in mouse somitogenesis. *Development* 134, 4033-41.

White, P. H. and Chapman, D. L. (2005). Dll1 is a downstream target of Tbx6 in the paraxial mesoderm. *Genesis* 42, 193-202.

Wittler, L., Shin, E. H., Grote, P., Kispert, A., Beckers, A., Gossler, A., Werber, M. and Herrmann, B. G. (2007). Expression of Msgn1 in the presomitic mesoderm is controlled by synergism of WNT signalling and Tbx6. *EMBO Rep* 8, 784-9.

Xu, X., Qiao, W., Li, C. and Deng, C. X. (2002). Generation of Fgfr1 conditional knockout mice. *Genesis* 32, 85-6.

Yasuhiko, Y., Haraguchi, S., Kitajima, S., Takahashi, Y., Kanno, J. and Saga, Y. (2006). Tbx6-mediated Notch signaling controls somite-specific Mesp2 expression. *Proc Natl Acad Sci U S A* 103, 3651-6.

Zhang, N. and Gridley, T. (1998). Defects in somite formation in lunatic fringe-deficient mice. *Nature* 394, 374-7.

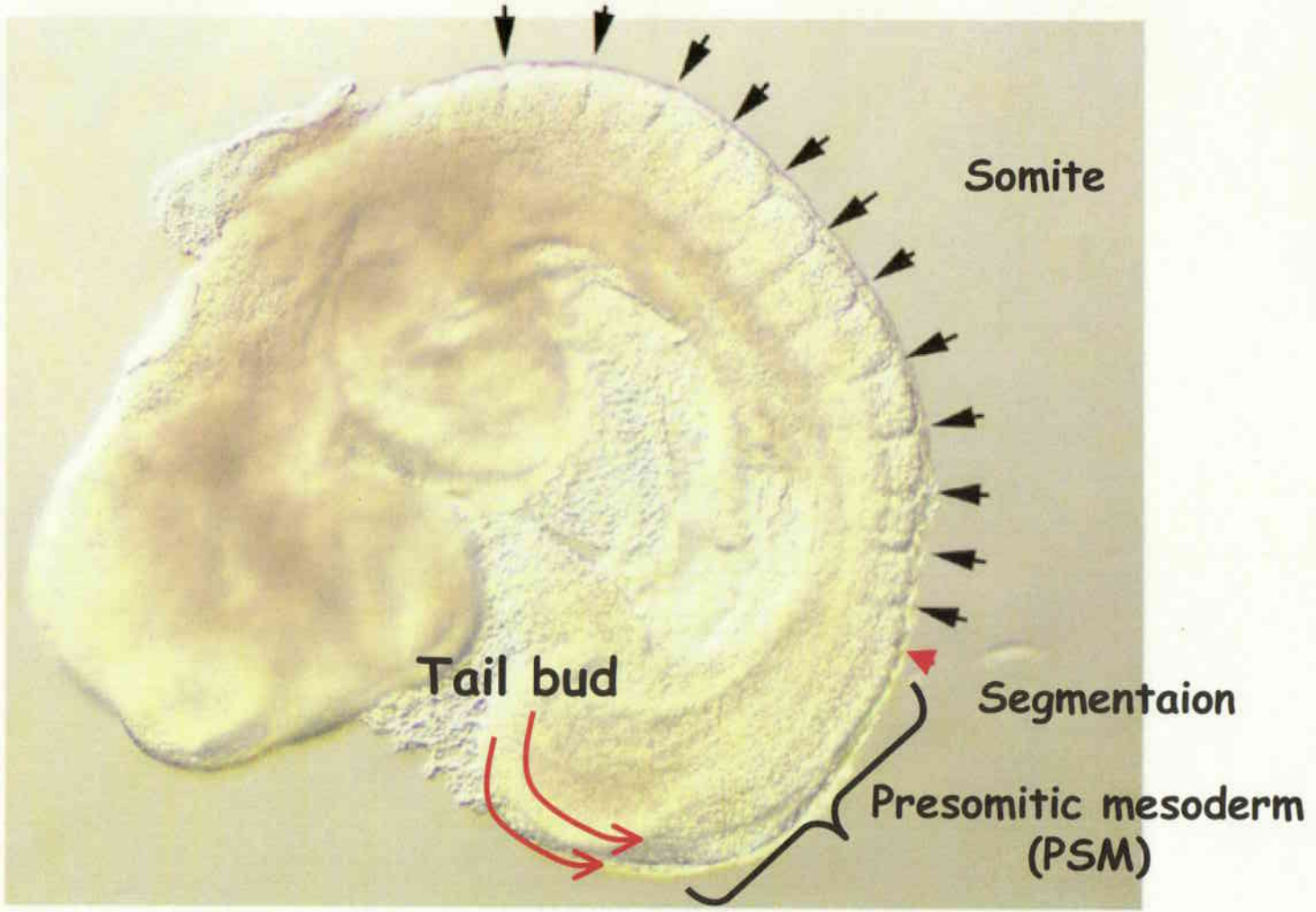

Figure 1. Somitogenesis in a mouse embryo at E9.0

Epithelial somites bud off sequentially from the rostral end of presomitic mesoderm (PSM), while more PSM cells are supplied from the paraxial mesoderm in the caudal region of the tail bud (shown by red arrows). Somites are generated every 2 hours in the mouse. Black arrows indicate formed somite borders, and the next presumptive border is indicated by a red arrowhead.

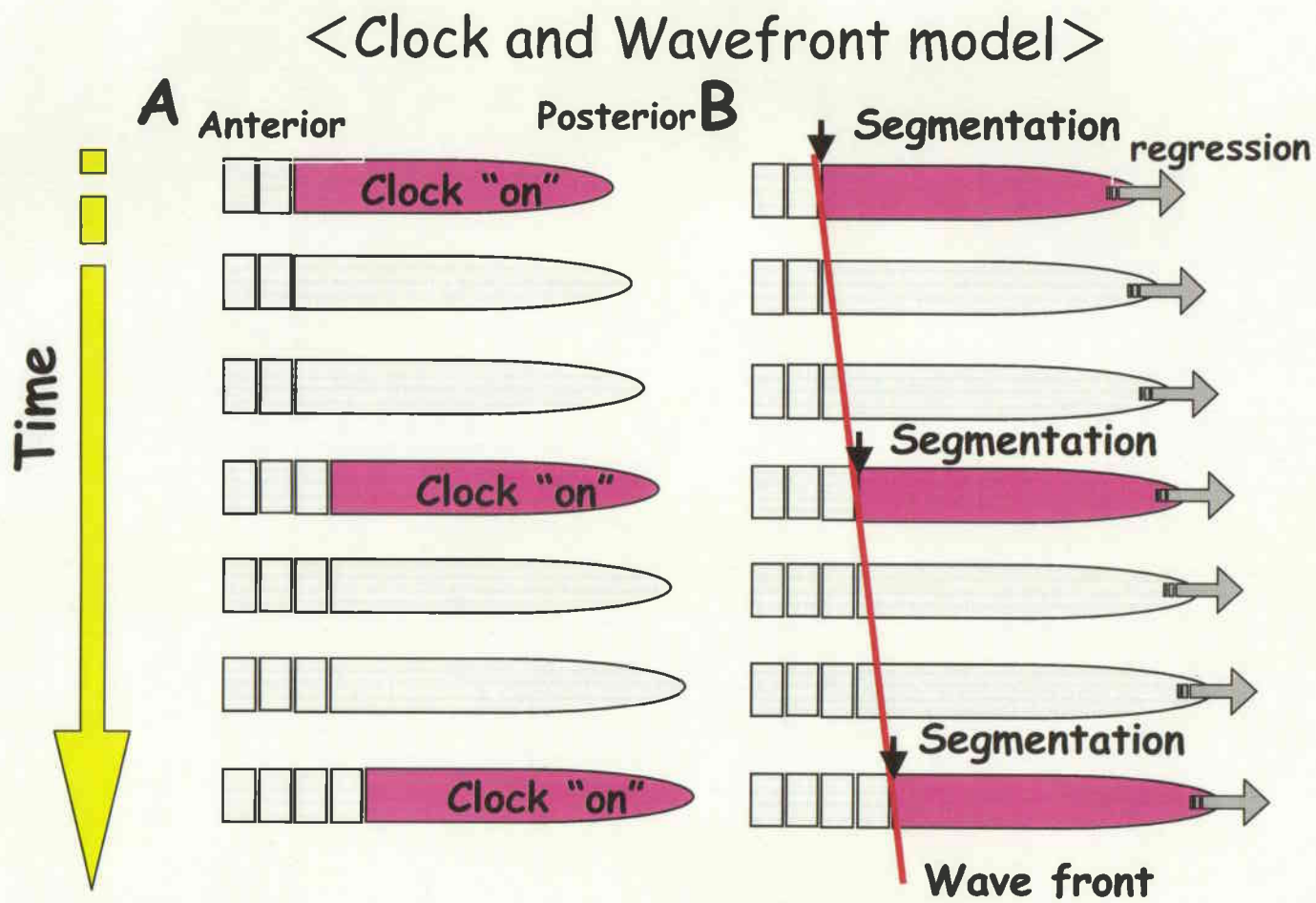

Figure 2. Clock & wavefront model

The "clock & wavefront model" is a model that helps to explain the sequential generation of the somite by the interaction of two hypothetical elements, a phase-linked oscillator that functions in the PSM and provides a base of periodicity of somitogenesis **(A)**, and a regressing "wavefront", which exists at the constant distance from the end of the tail bud **(B)**. In this model, oscillating cells set their output when they

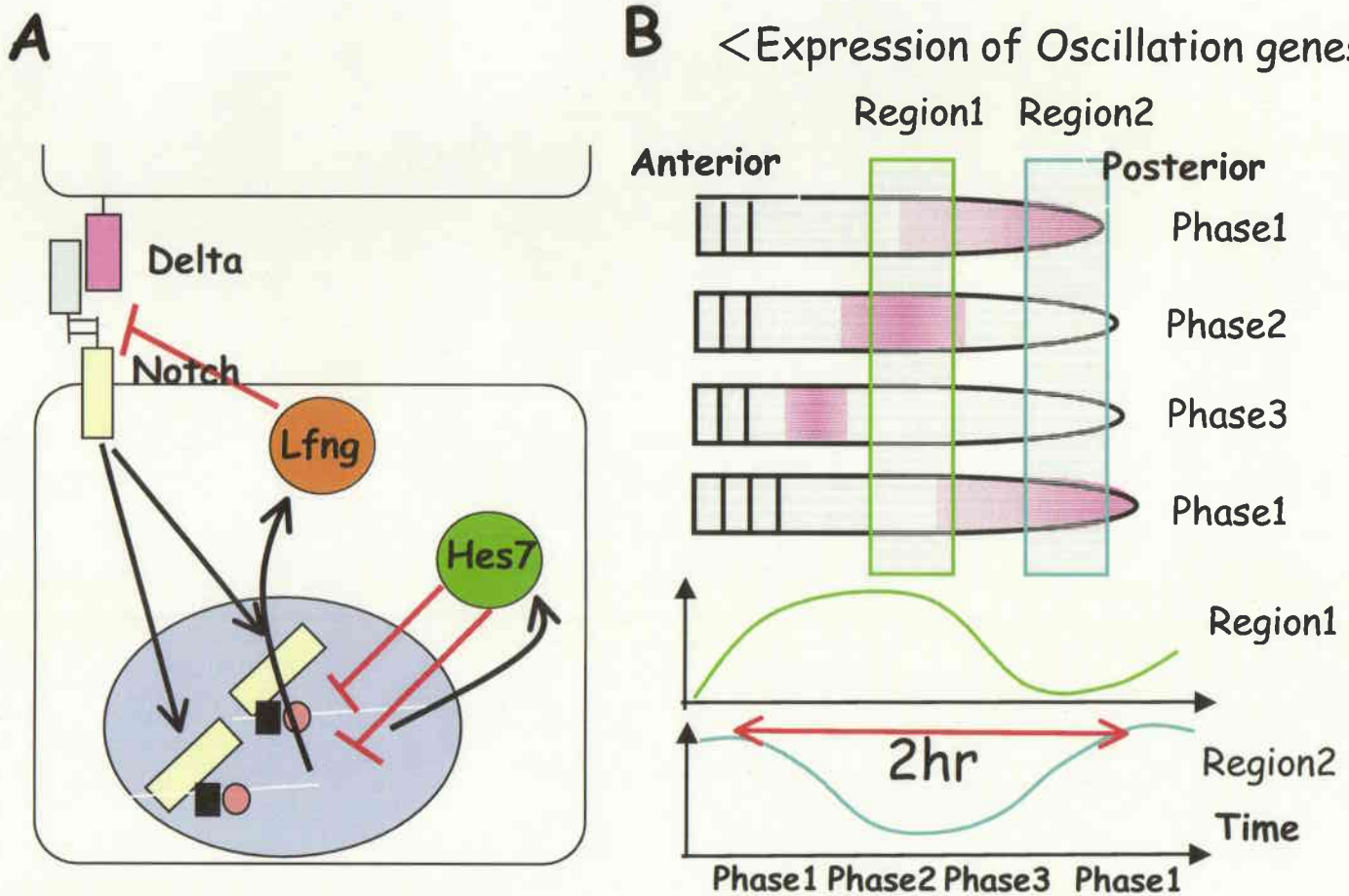

Figure 3. The mechanism of Notch signal oscillation

(A) Oscillatory expressions of Notch target genes are regulated by negative feedback mechanisms. Notch signaling induces transcription of *Hes7* and *Lfng*. The translated Hes7 protein may directly bind to promoters of *Hes7* and *lfng* to repress their transcription, while Lfng protein represses Notch signaling through suppressing interaction between Dll (ligand) and Notch (receptor).**(B)** Oscillation of Notch target genes in the PSM during somitogenesis. Expression of oscillation genes periodically propagates like a wave, from the posterior end of the PSM to the anterior region, and each wave cycle links to the generation of one somite. This dynamic change is elicited by oscillatory expression in each PSM cell with a slight delay from the posterior to anterior direction.

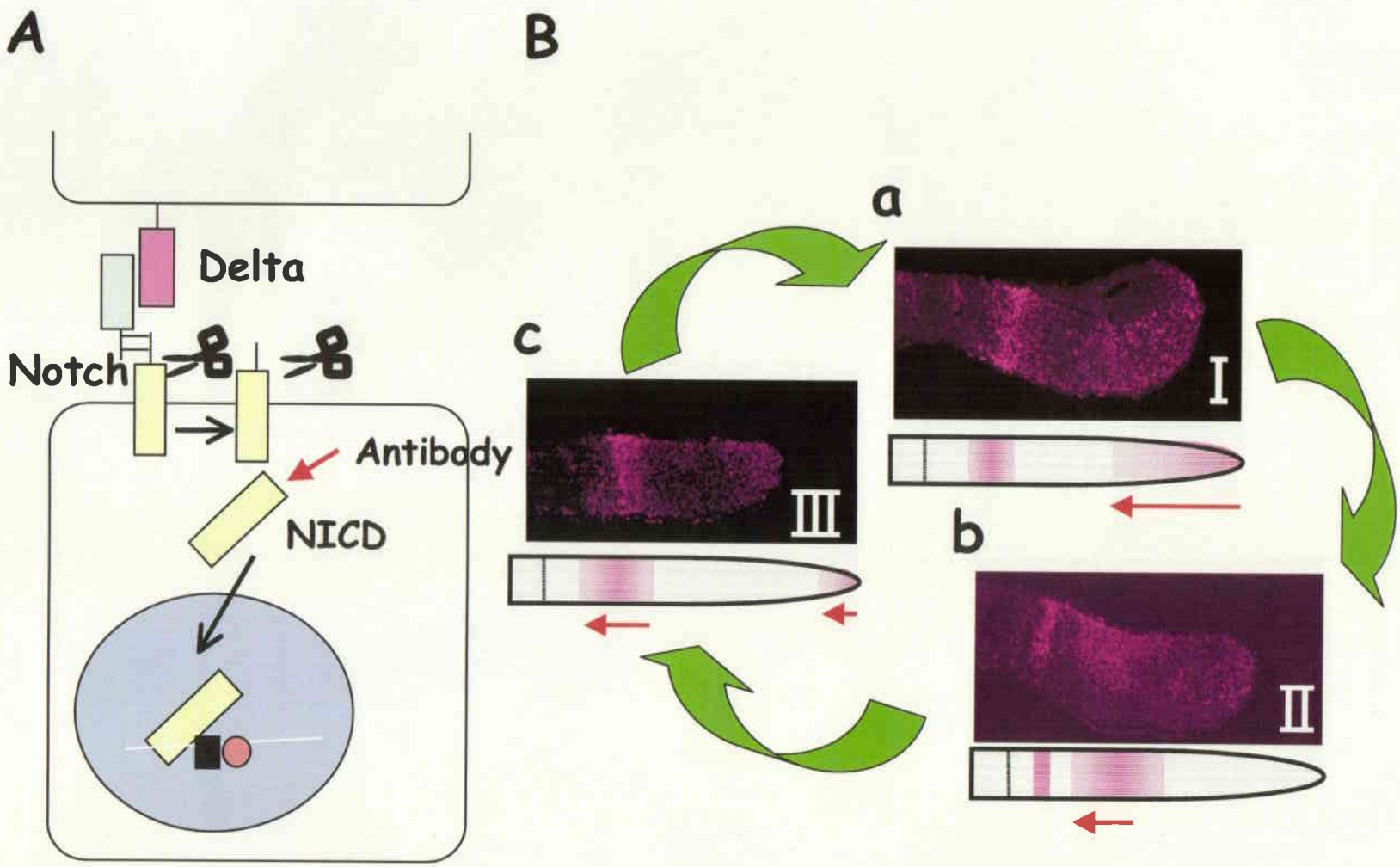

Figure 4. Visualization of the Notch signal activity in mouse somitogenesis

(A) The Notch signaling pathway and the specificity of an antibody used for monitoring the Notch activity are depicted. The antibody recognizes only a processed form of Notch receptor, NICD (Notch intracellular domain). **(B)** A Notch standard time (I-III) was defined by the location of the Notch active domain in the posterior PSM. The wave of oscillating Notch activity is born at the end of posterior PSM in phase-I **(a)**. The oscillating Notch activity moves to the intermediate region of PSM in phase-II **(b)**. The Notch activity reaches the anterior PSM in Phase-III **(c)**.

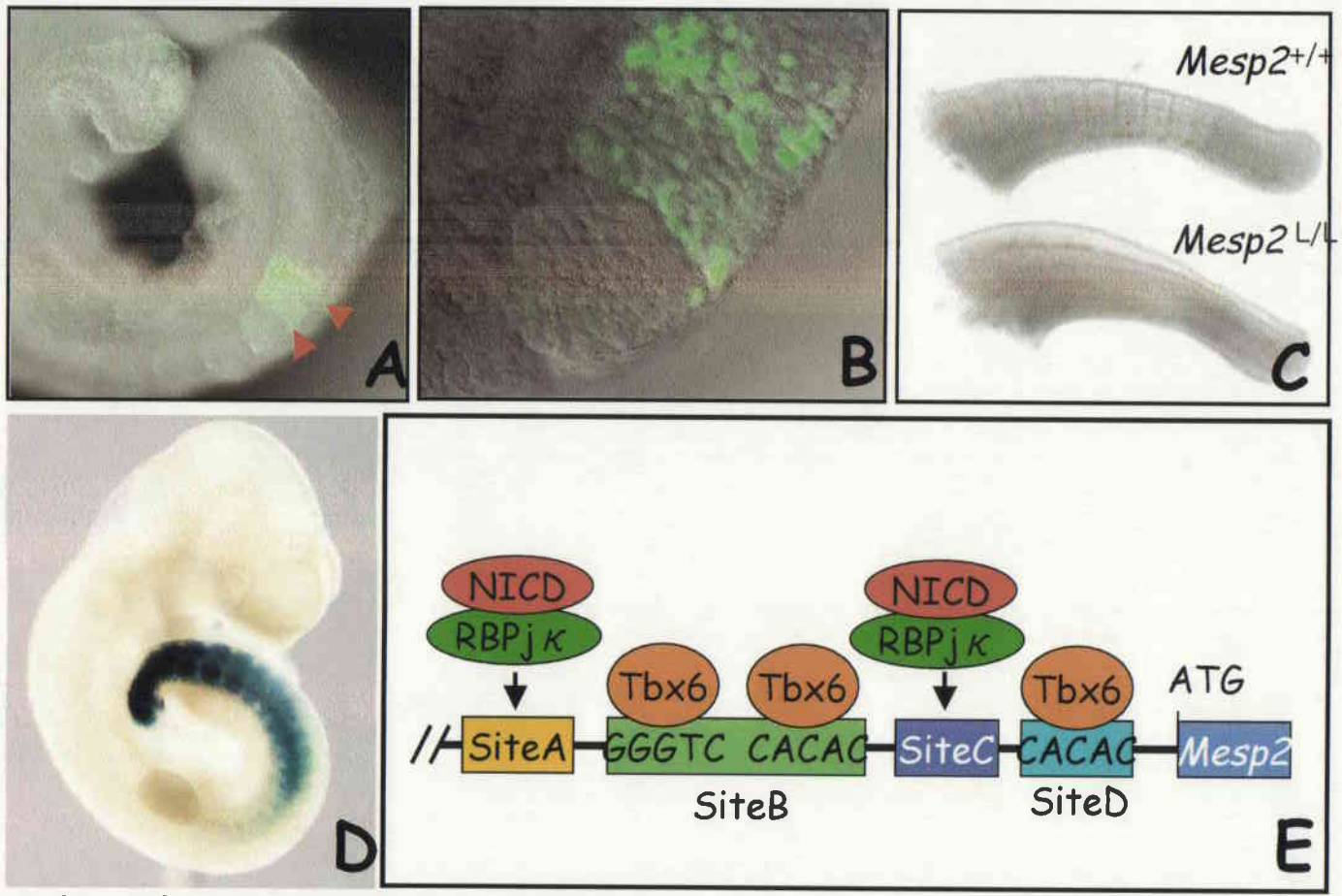

Figure 5. Expression and function of Mesp2 in mouse somitogenesis

(A, B) The expression of Mesp2-Venus fusion protein at E8.75. **(B)** The higher magnification image of **(A)**. Red arrowheads indicate anterior limits of Mesp2-Venus, which corresponds to the segmental border. **(C)** The segmental border is not created in the Mesp2-null mouse. **(D)** A LacZ staining pattern of a transgenic mouse embryo harboring a Mesp2 enhancer, the 185-bp upstream region of 5' flanking region of the *Mesp2* gene. **(E)** A model for the mechanism underlying Mesp2 transcription. Tbx6 and NICD interact with the upstream enhancer sites (site A-D) of the *Mesp2* gene. Sites A and C interact with a Notch signal mediator, RBPjk and up-regulate *Mesp2* expression in the presence of NICD. This activation fully depends on the binding of Tbx6 to Sites B and D.

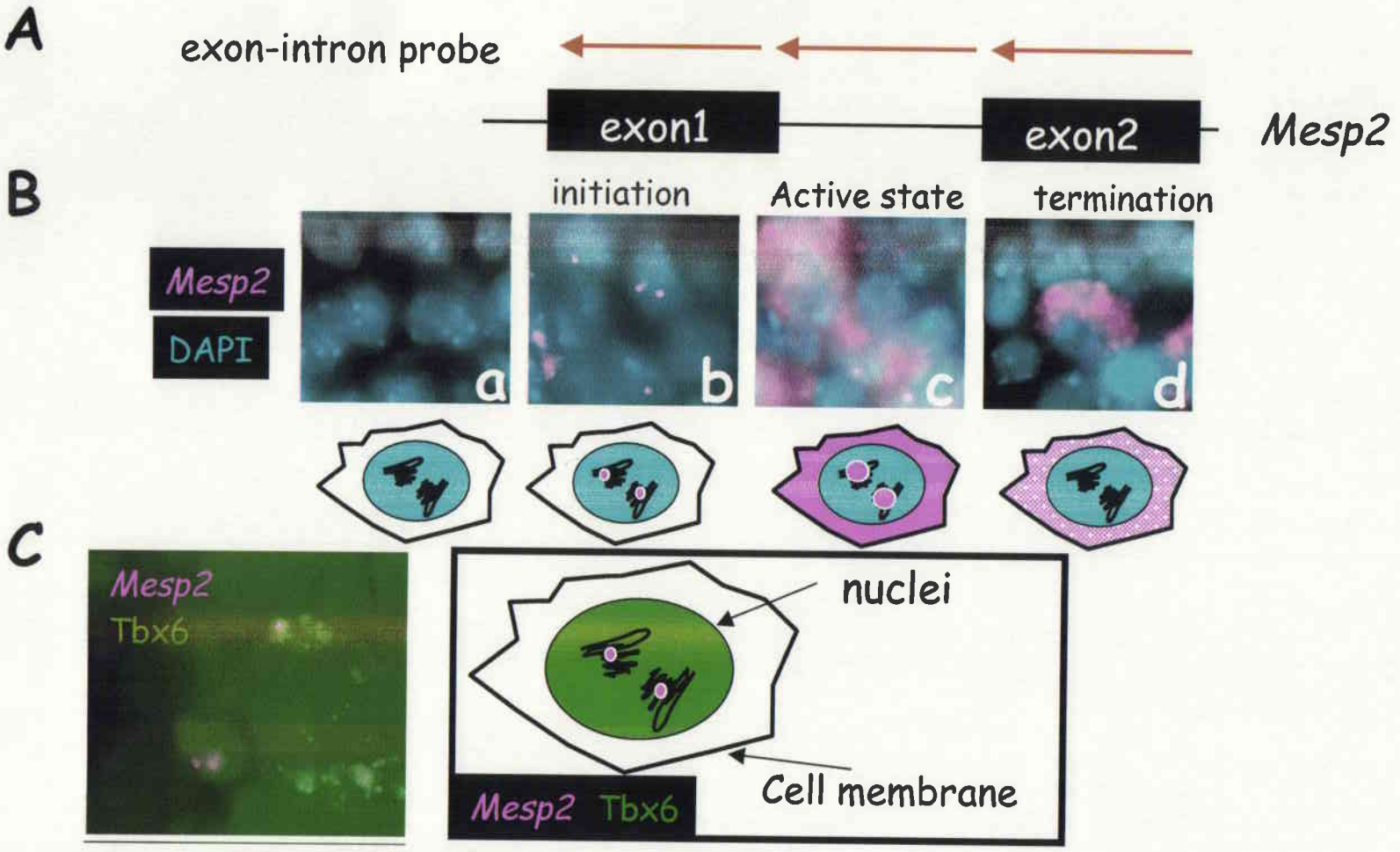

Figure 6. Strategies to visualize *Mesp2* transcription in mouse somitogenesis

(A) A schematic presentation of *Mesp2* probes used for in situ hybridization. **(B)** Representative *Mesp2* transcription states revealed by high resolution in situ hybridization with combined antisense probes corresponding to an intronic region and exons of *Mesp2*. (**a**) no transcription, (**b**) primary transcription, (**c**) active transcription and cytoplasmic accumulation of transcripts, and (**d**) transcriptional termination. Magenta; *Mesp2* transcripts, Blue; DAPI staining. **(C)** An example of successful visualization of *Mesp2* transcription and Tbx6 protein by high-resolution fluorescent in situ hybridization using intronic probes together with immunostaining to detect Tbx6 using Tbx6 antibody.

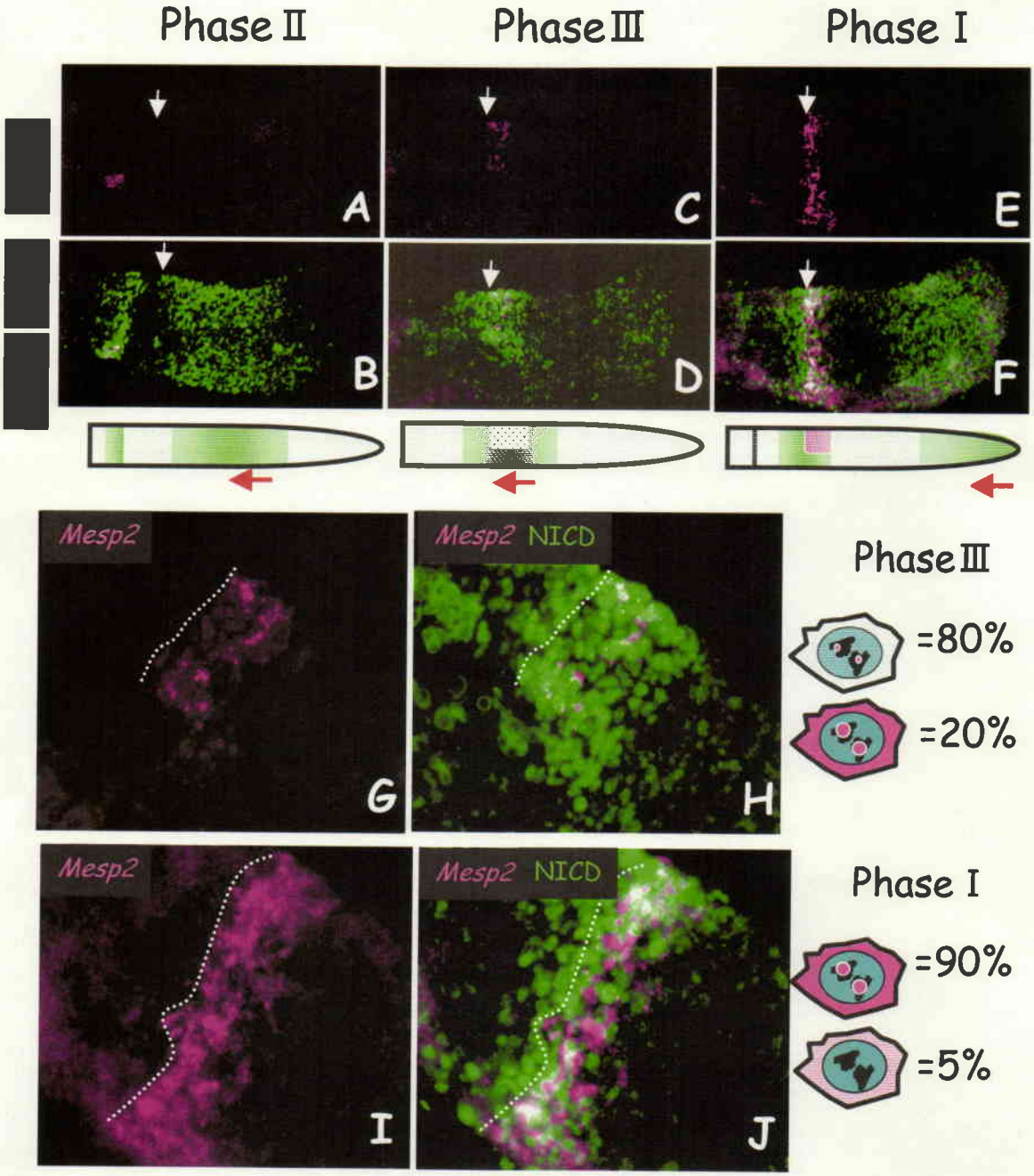

Figure 7. The temporal regulation of *Mesp2* transcription by Notch signaling.

Double staining of *Mesp2* transcripts (in situ hybridization) and Notch activity (anti-NICD antibody) during one cycle of somitogenesis. *Mesp2* transcription was not detected in phase-II (**A, B**), was found to be initiated during phase-III (**C, D**), and was further up-regulated in phase-I (**E, F**). Arrowheads in **(A-F)** indicate anterior limits of *Mesp2* transcription. **(G-J)** Higher magnification images of phase-III (**G, H**) and phase I (**I, J**) are shown. *Mesp2* transcripts were detectable in the posterior half of the Notch active domain with a clear anterior boundary (shown by dotted lines in **G-J**). The estimated relative ratios for cells showing different subcellular localizations of *Mesp2* transcripts are shown on the right of the panels for phase-III and -I.

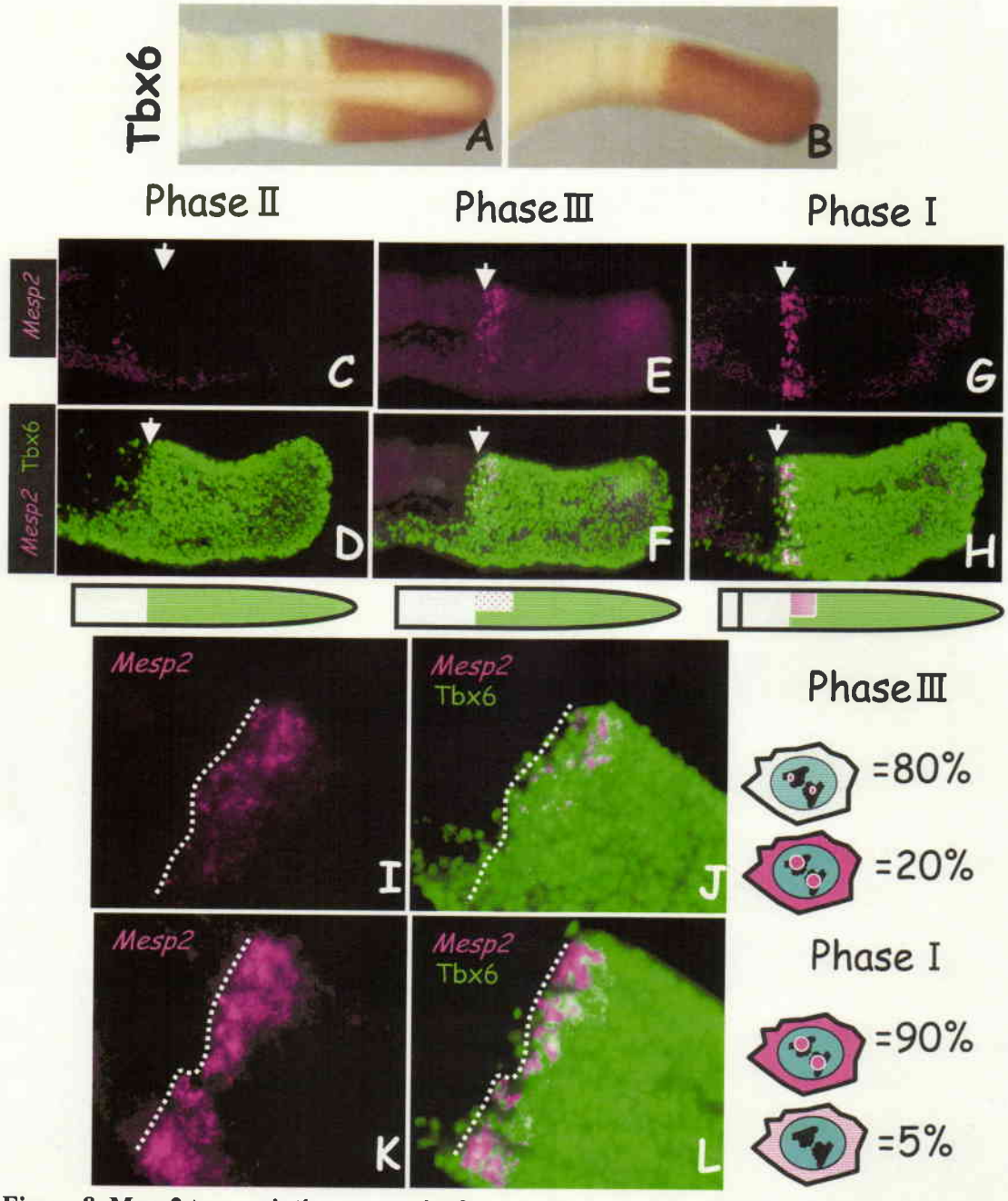

Figure 8. Mesp2 transcription occurs in the anterior end of the Tbx6 expressing domain.

(A, B) Whole mount immunostaining with anti-Tbx6 antibodies indicates a clear anterior border of Tbx6 protein in the dorsal view (**A**) and lateral view **(B). (C-H)** Double staining of *Mesp2* and Tbx6 was conducted using a single embryo for each phase (**C, D**, phase-II) (**E, F**, phase-III) and (**G, H**, phase-I). The anterior border of Tbx6 protein is perfectly matched with that of *Mesp2* transcription, in either phase-III **(E, F)** or phase-I (**G, H**), when *Mesp2* transcription is detectable. Arrowheads in **(C-H)** indicate anterior limits of *Mesp2* transcription. **(I-L)** Higher magnification images of phase-III (**I, J**) and phase I (**K, L**). The anterior border of *Mesp2* transcripts (shown by dotted lines in **I-L**) were perfectly matched with the anterior border of Tbx6 protein. The transcriptional states in panels were roughly estimated using the subcellular localization pattern of the *Mesp2* transcripts and are

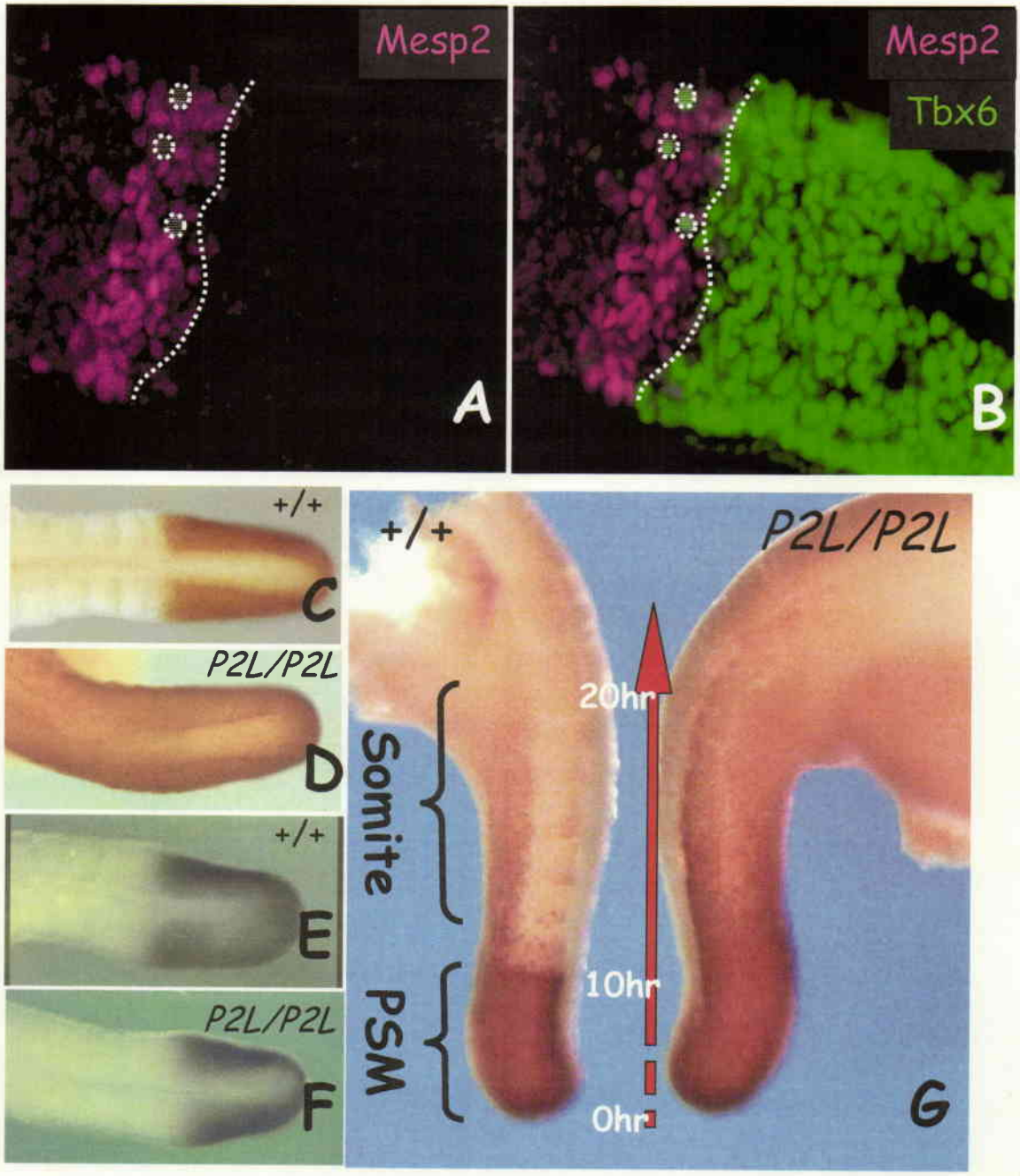

Figure 9. Mesp2 suppresses Tbx6 protein expression.

(A, B) Double immunostaining of Mesp2 and Tbx6 proteins. These two expression domains are segregated and form a clear border (indicated by the dashed lines). Some cells were found to still express Tbx6 in the Mesp2 expression domain but lacked Mesp2 expression (indicated by the dotted circles). **(C-F)** Comparison of the expression patterns for Tbx6 protein **(C, D)** and mRNA **(E, F)** between wild-type (+/+) and Mesp2-null mice (P2L/P2L). The stability of Tbx6 was compared in embryonic tails with or without Mesp2 **(G)**. The time was estimated by the number of somites formed in the wild-type embryo.

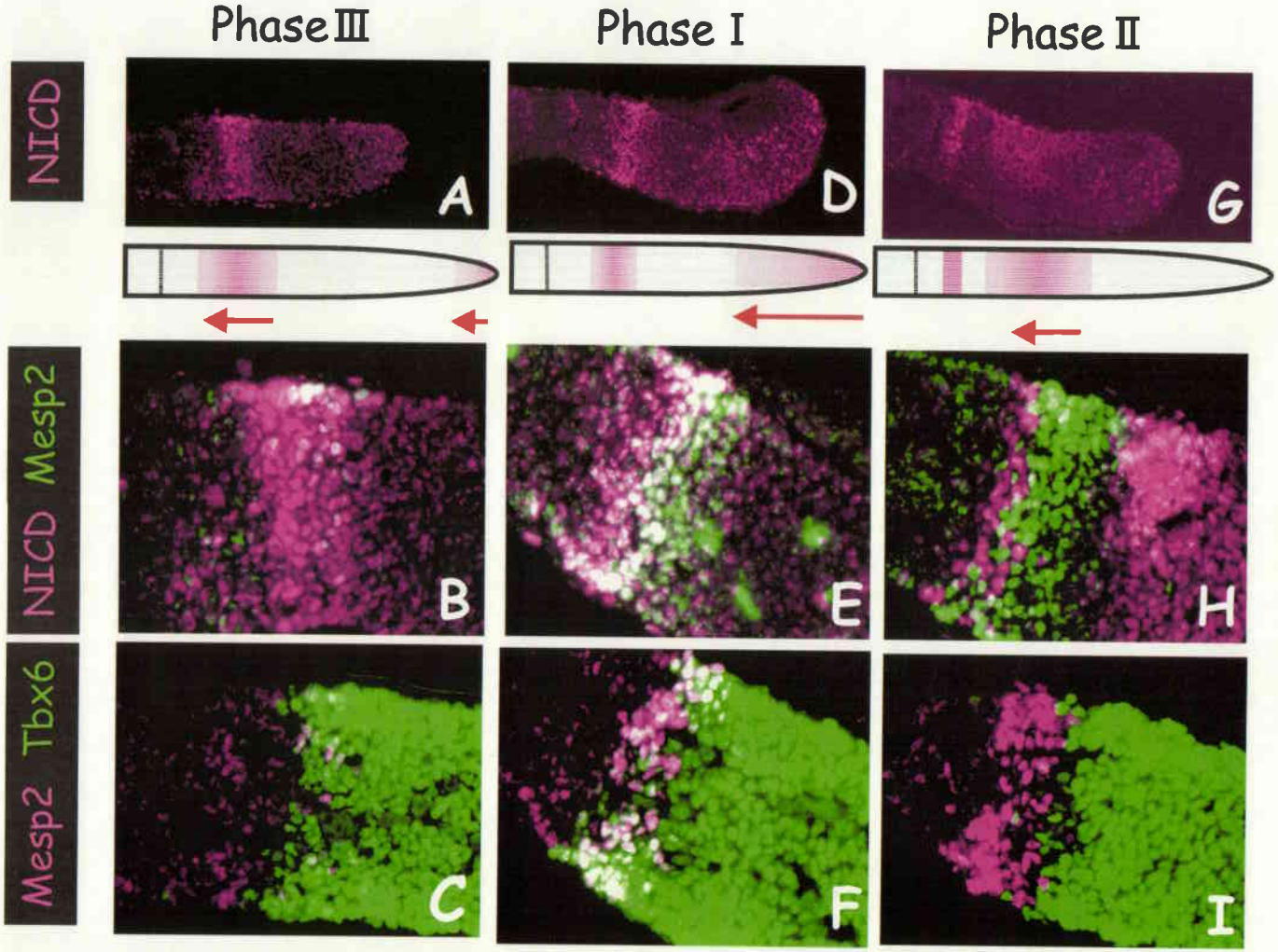

Figure 10. The spatio-temporal dynamics of Mesp2, Tbx6 and Notch activity during somitogenesis.

(A-I) Double immunostaining patterns that are representative of the relationships between Mesp2, Tbx6 and Notch during somitogenesis. The stained sections shown in the vertical rows are derived from a single embryo. The pattern of Notch activity shown in the top panels **(A, D, G)** was used to assign the phase (only a single channel for Notch activity is shown). The factors being detected are indicated in the left panels. Anterior is to the left.

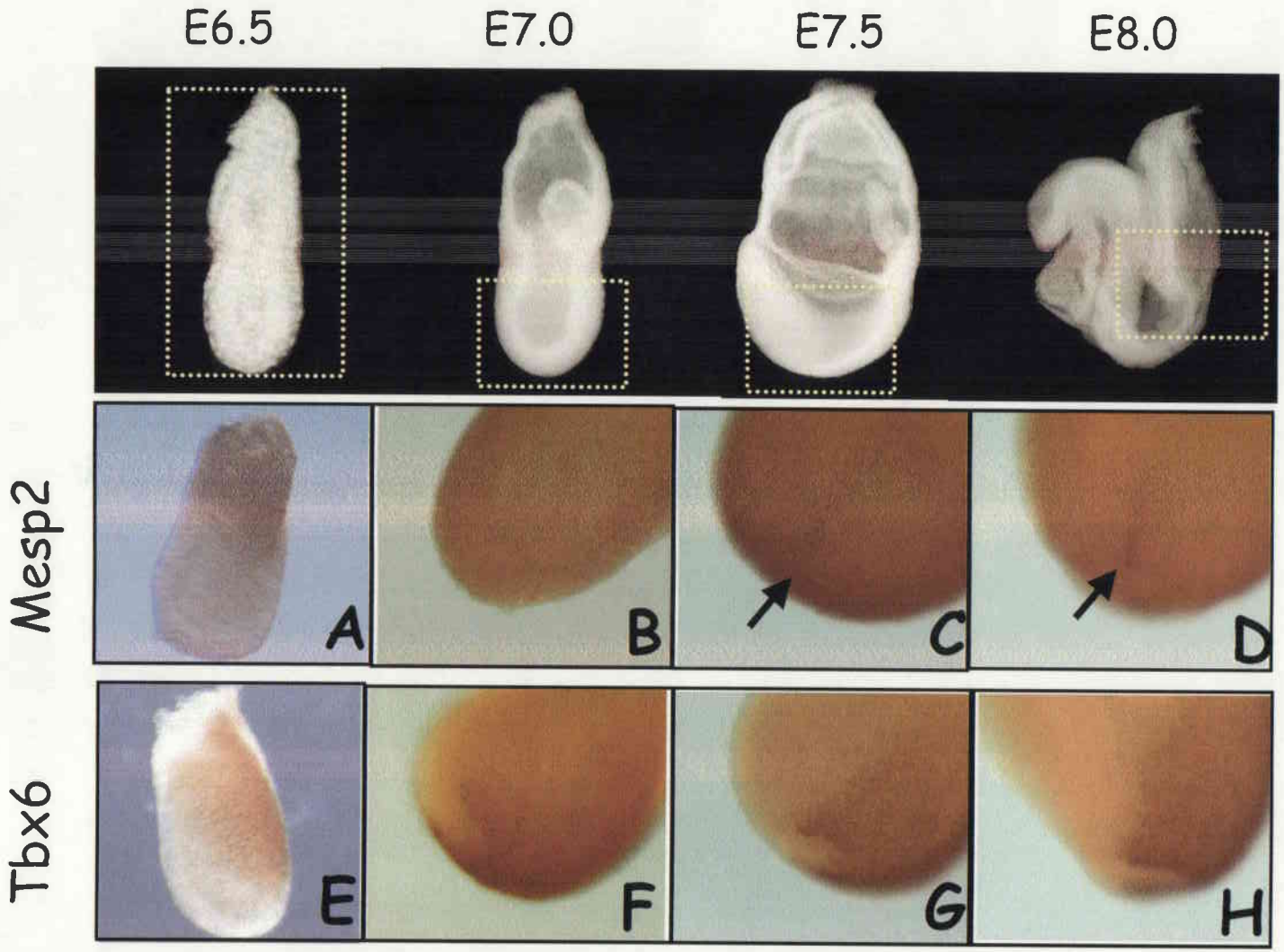

Figure 11. Expressions of Mesp2 and Tbx6 in early stage embryos from E6.5 to E8.0.

(A-D) Expression of Mesp2 protein starts from E7.5.Arrows indicate expression of Mesp2. **(E-H)** Embryos from E6.5 to E7.0 showed graded expression of Tbx6 protein without clear anterior limit **(E, F)**, while embryos from E7.5 to E8.0 showed the expression with the anterior border **(G, H)**.

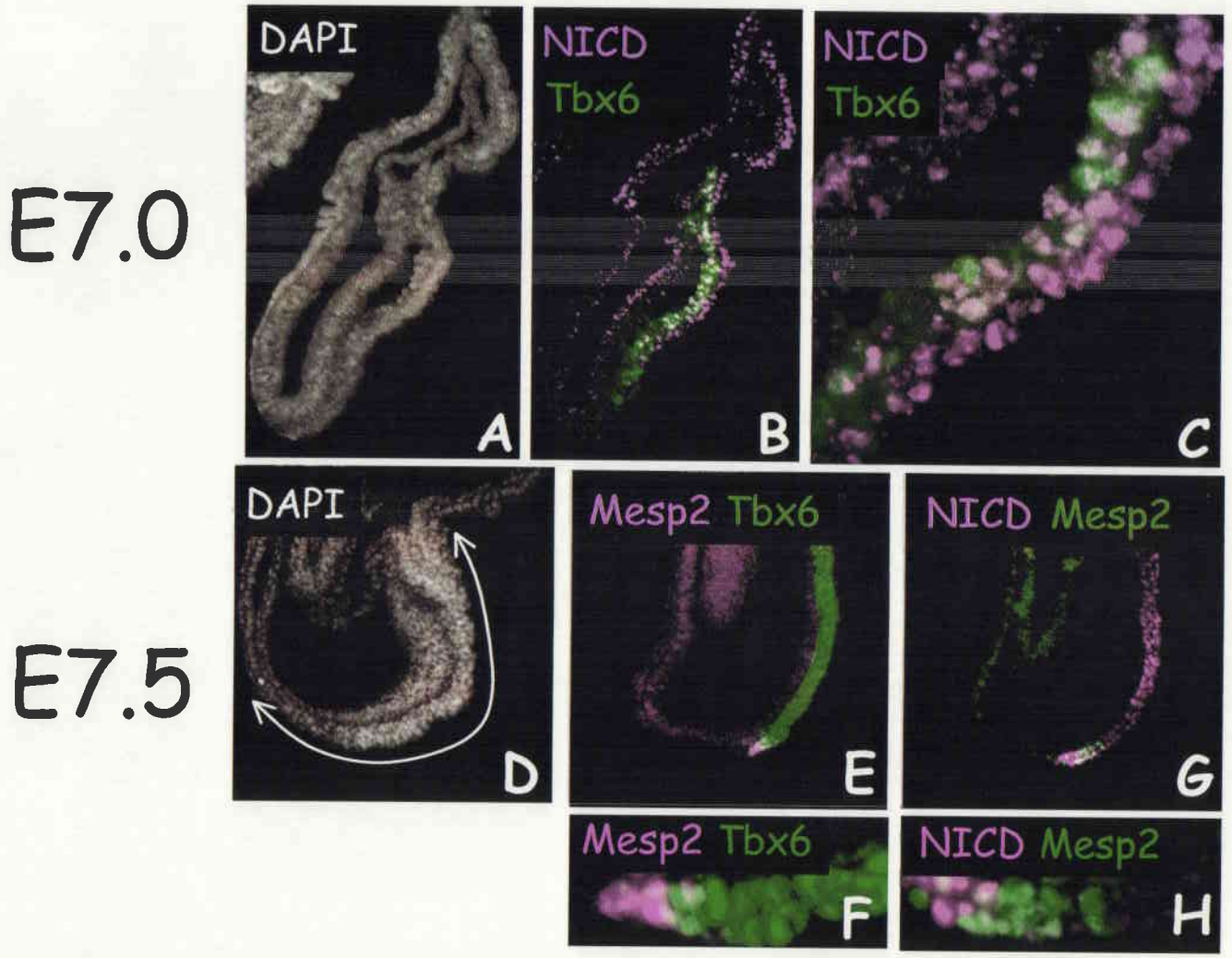

Figure 12. The spatio-temporal dynamics of Mesp2, Tbx6 and Notch activity during late-streak stage

(A-C) Sections of an early stage embryo (around E7.0) stained with DAPI **(A)**, and with antibodies against NICD and Tbx6 **(B, C).** A higher magnification image of (**B**) is shown in **(C). (D-H)** Analyses of late-streak stage embryos just prior to somite formation (around E7.5). Stained sections indicating the embryonic structure by DAPI staining (**D**), and double stained with Tbx6 and Mesp2 (**E, F**), and Mesp2 and NICD (**G, H**) are shown. Higher magnification images for (**E**) and (**G**) are shown in (**F**) and (**H**), respectively.

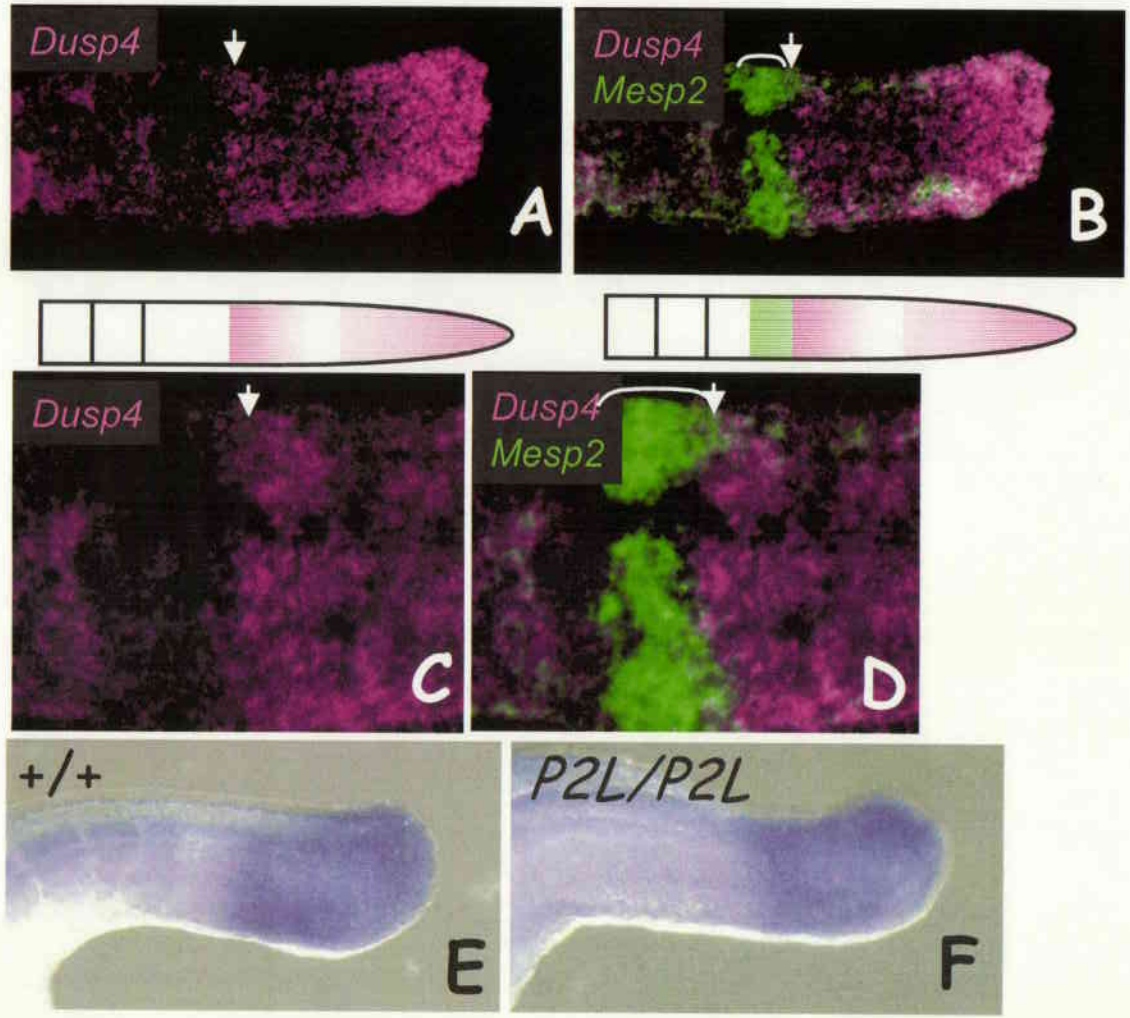

Figure 13. Expressions of *Mesp2*, and *Dusp4* that is one of the downstream targets of FGF signaling

(A-D) The spatial relationship between *Mesp2* and *Dusp4* was examined by double in situ hybridization. The posterior border of the *Mesp2* expression domain (indicated by a round bracket in **B, D**) is matched with the anterior limit of the *Dusp4* expression domain (the border is indicated by the arrow in **A-D**). **(C, D)** Higher magnification images of **(A, B)**. **(E, F)** *Dusp4* expression revealed by whole mount in situ hybridization in wild-type **(E)** and Mesp2-null **(F)** embryos.

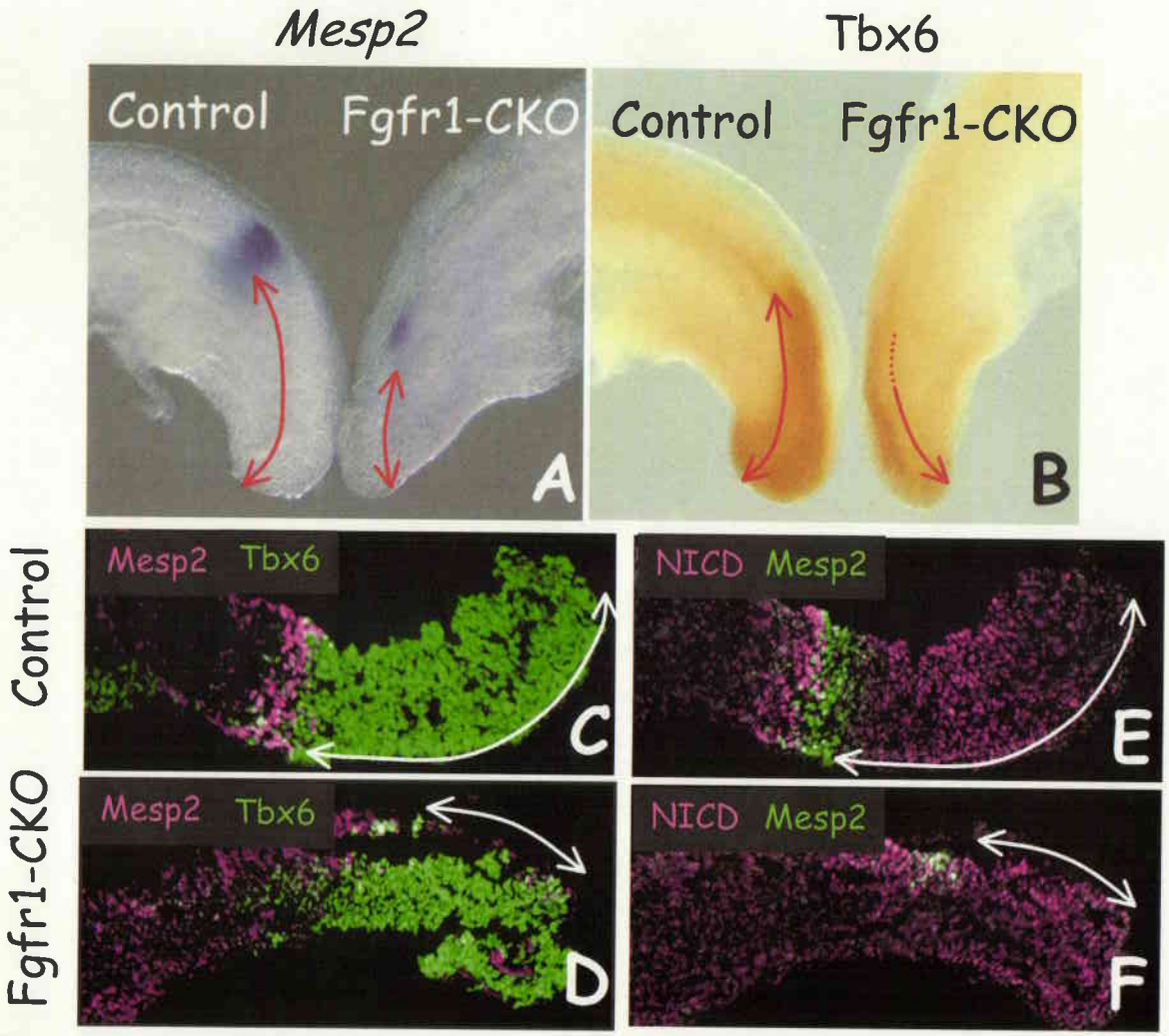

Figure 14. Effects of the lack of FGF signaling upon the regulation of *Mesp2* expression pattern

(A-F) Comparison of the *Mesp2* expression pattern between in the wild-type and a PSM-specific Fgfr1-knockout embryo. Whole mount in situ hybridization revealed a posterior shift of the *Mesp2* expression domain in the Fgfr1-cKO embryo (**A**). Whole mount immunostaining with anti-Tbx6 antibodies indicated an ambiguous anterior border in the Fgfr1-cKO embryo **(B).** The section double immunostaining was employed to examine Tbx6 and Mesp2 (**C, D**) or Mesp2 and NICD (**E, F**) in both wild-type control (**C, E**) and Fgfr1-cKO (**D, F**) embryos.

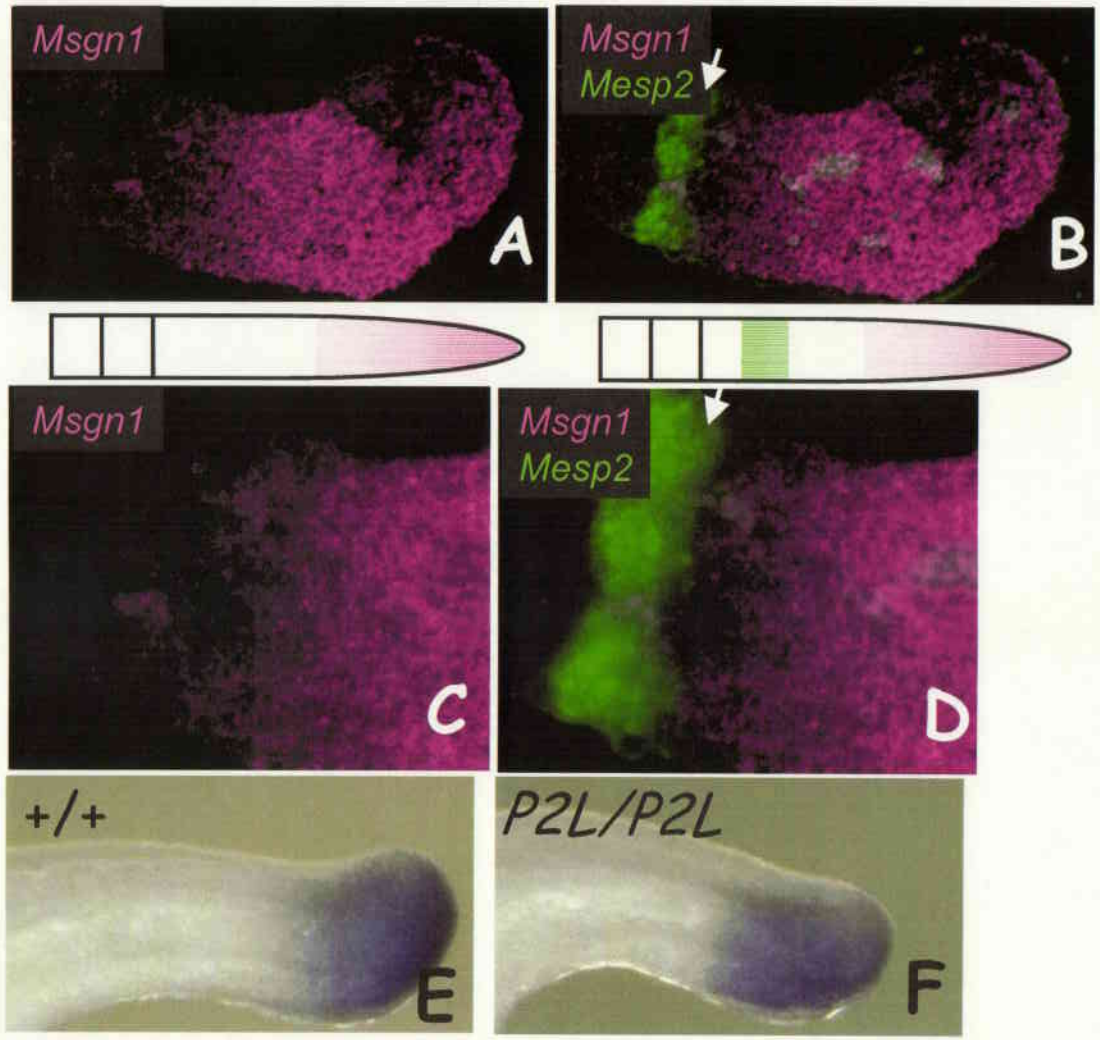

Figure 15. Mesp2 expression is not directly regulated by Wnt signaling.

(A-D) The spatial relationship between *Mesp2* (green) and *Mesogenis1* (*Msgn1*, magenta) expressions. Arrows indicate posterior limits of *Mesp2* transcription. **(C, D)** Higher magnification images of **(A, B)**. **(E, F)** *Msgn1* expression revealed by whole mount in situ hybridization in wild-type **(E)** and Mesp2-null **(F)** embryos.

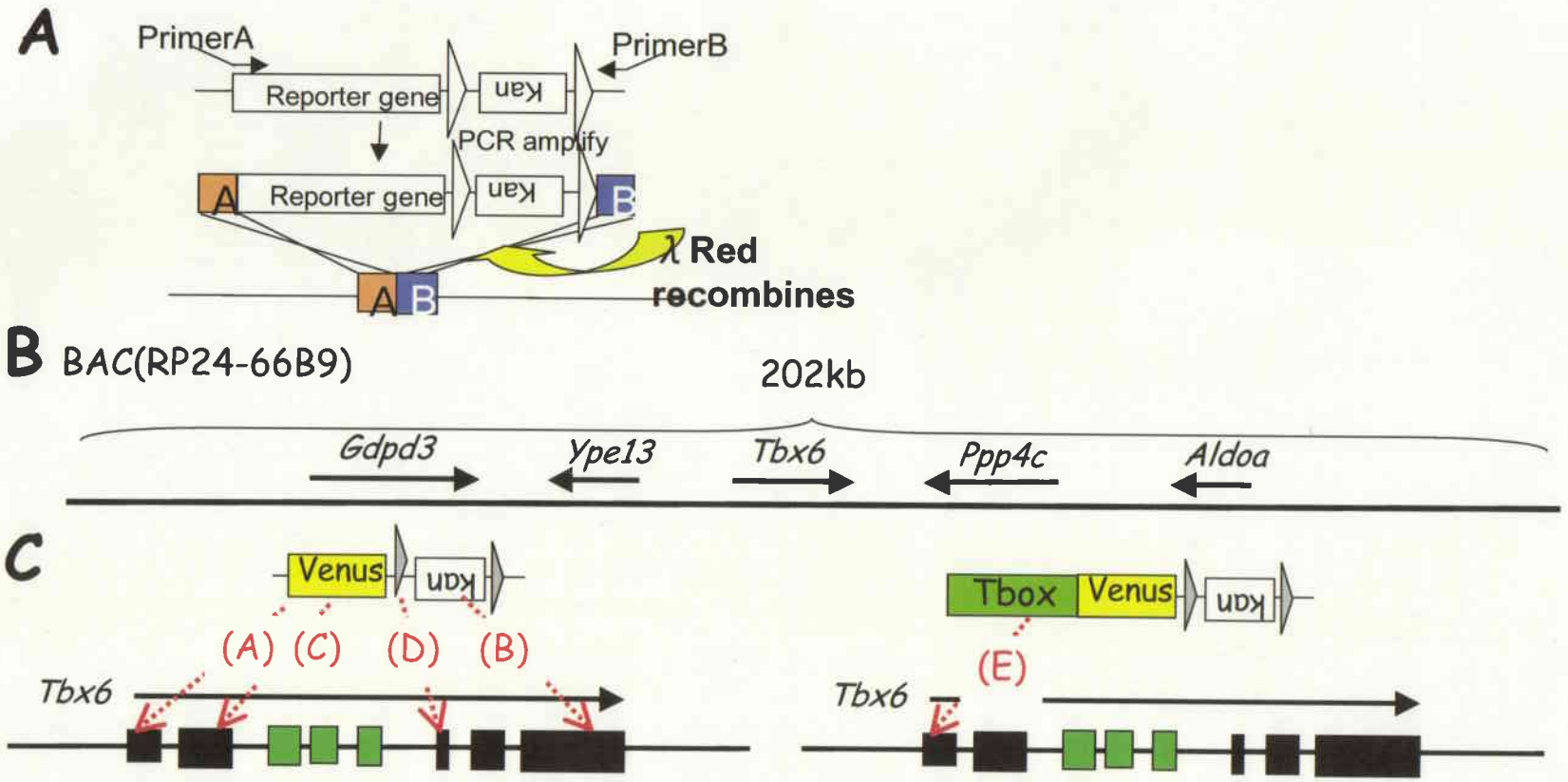

Figure 16. BAC modification strategy and its application to a BAC clone containing the *Tbx6* gene

(A) Schematic representation of the BAC modification method used in this study, which utilized a gene cassette harboring a kanamycin resistance gene flanked by two FRT sequences. The DNA fragment required for homologous recombination was generated by PCR using Primer A and Primer B, which contain genomic sequences A and B, respectively. The reporter gene containing the kanamycin cassette was then introduced into a BAC clone using the λRed recombination system. **(B)** Gene organization of a BAC clone containing the *Tbx6* gene. **(C)** Strategies to generate BAC constructs with Venus-tag at different positions of Tbx6 protein. The venus-tag was introduced in frame with either translational initiation site (A, BAC-Venus), translational termination site (B, BAC-Tbx6-Venus), before T-box (C, BAC-Tbx6 Δ CT-Venus) or after T-box (D, BAC-Tbx6 Δ C-Venus). The method was also used to generate a construct containing only T-box with Venus (E, BAC-Tbox-Venus). Black and green boxes indicate exons of Tbx6 locus. Green ones correspond to the T-box region.

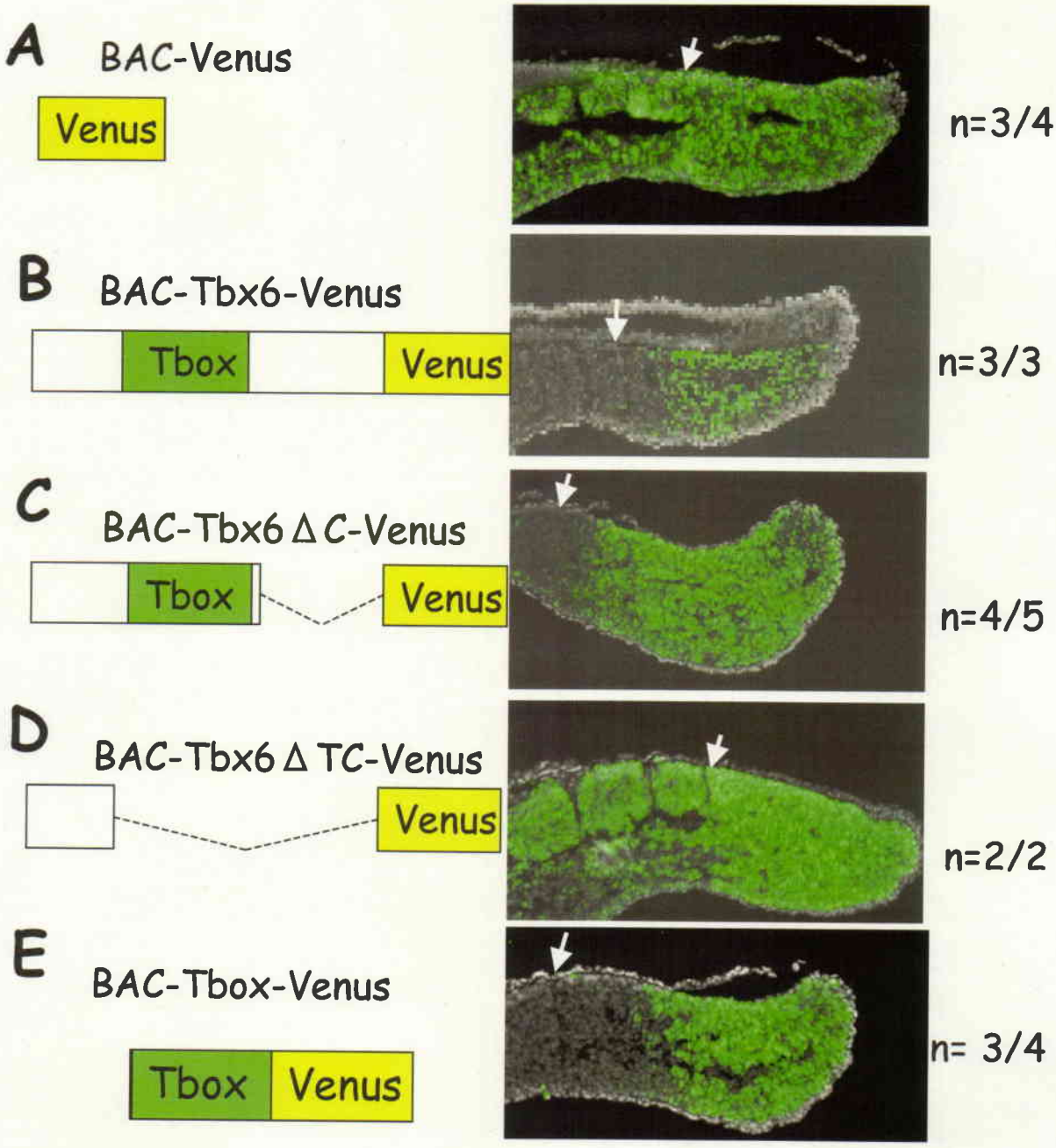

Figure 17. T-box is essential and sufficient for Tbx6 to be suppressed.

Sections of transient transgenic mouse embryos harboring each BAC construct (indicated in the left) were stained with anti-venus antibody. The numbers of Venus positive embryos among the total embryo cohorts that were obtained are indicated on the right. Transgenic mouse embryos harboring BAC-Venus **(A)** and BAC-Tbx6 Δ CT-Venus **(D)** showed expanded expressions, in which Venus proteins were retained at the somitic region. Those of BAC-Tbx6-Venus **(B),** BAC-Tbx6 Δ C-Venus **(C)** and BAC-Tbox-Venus **(E)** showed restricted expressions, in which Venus protein had clear anterior borders. Green; Venus, Gray; DAPI staining. Newly formed somite borders are shown by white arrowheads.

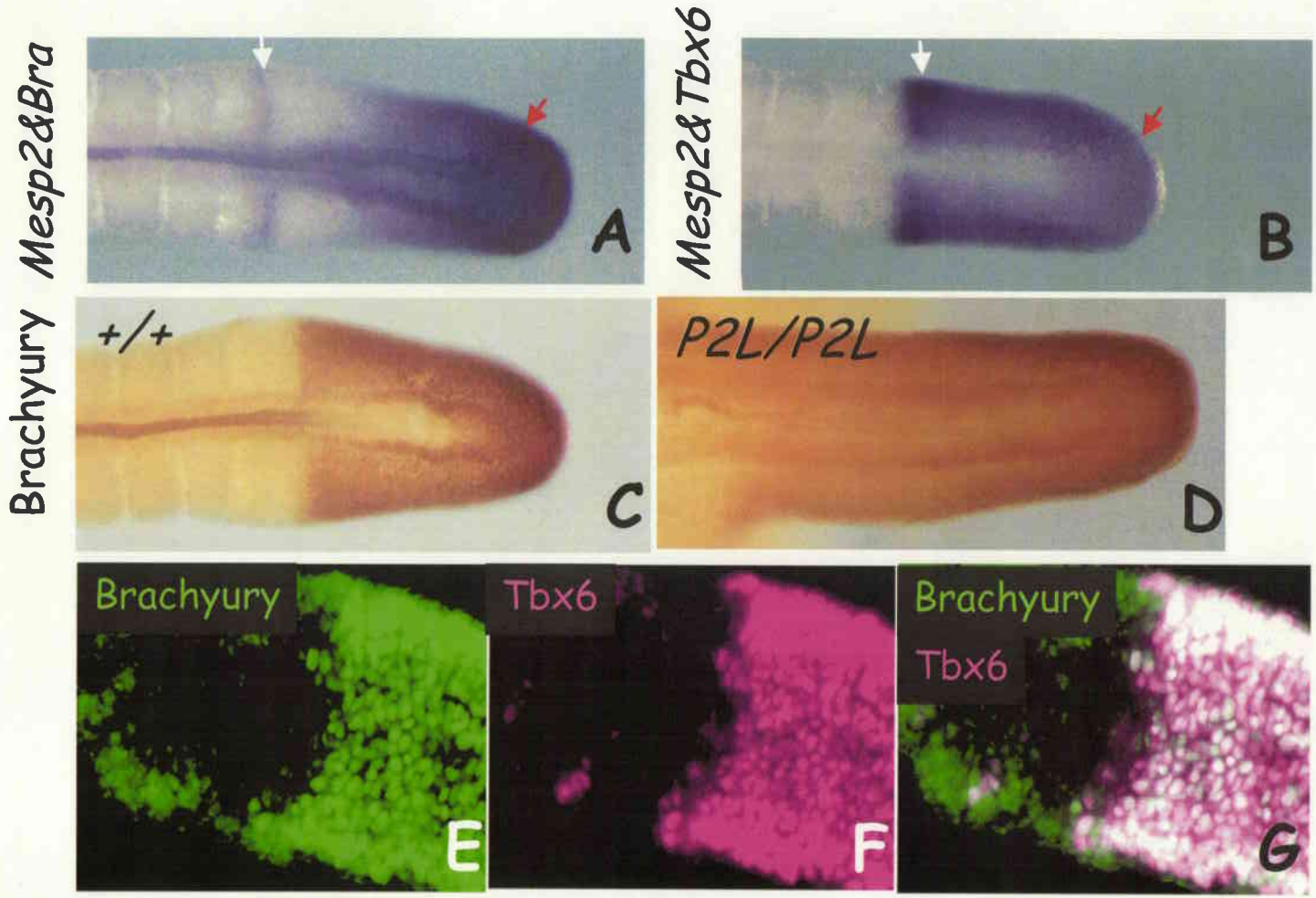

Figure 18. Mesp2 also suppresses Brachyury expression via posttranslational mechanism

(A, B) The mRNA localization of *Mesp2* and *Brachyury* **(A),** or *Mesp2* and *Tbx6* **(B)**, revealed by in situ hybridization using mixed antisense probes for *Mesp2* and *Brachyury* **(A)** or *Mesp2* and *Tbx6* **(B)**. Expressions of *Mesp2* are shown by white arrows. Expressions of *Brachyury* or *Tbx6* are shown by red arrows. **(C-D)** Comparison of the expression patterns for Brachyury protein between wild-type (+/+) **(C)** and Mesp2-null mice (P2L/P2L) **(D)**. **(E-G)** Double immunostaining pattern of Brachyury and Tbx6 proteins. The anterior border of Brachyury protein is

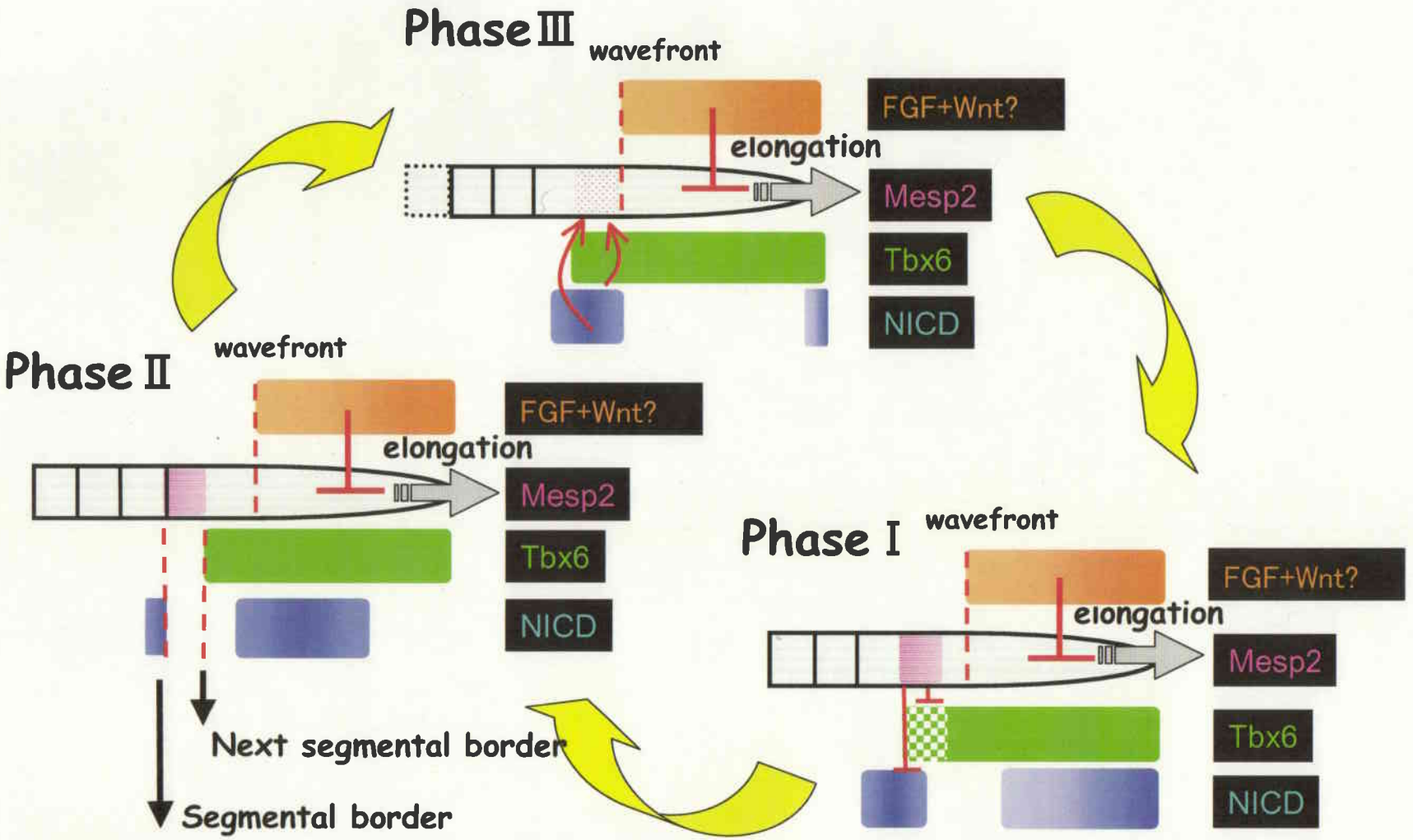

Figure 19. Proposed models for the molecular mechanisms to generate periodicity in somitogenesis

A schematic representation of the temporal and spatial changes in the expression patterns and relationships among Mesp2 (pink), Tbx6 (green), NICD (blue) and FGF signaling (orange) during a single cycle of somitogenesis. The FGF signal is provided from the end of the PSM with a posterior to anterior gradient. The expected threshold in the activity defines the determination wavefront that corresponds to the posterior limit of

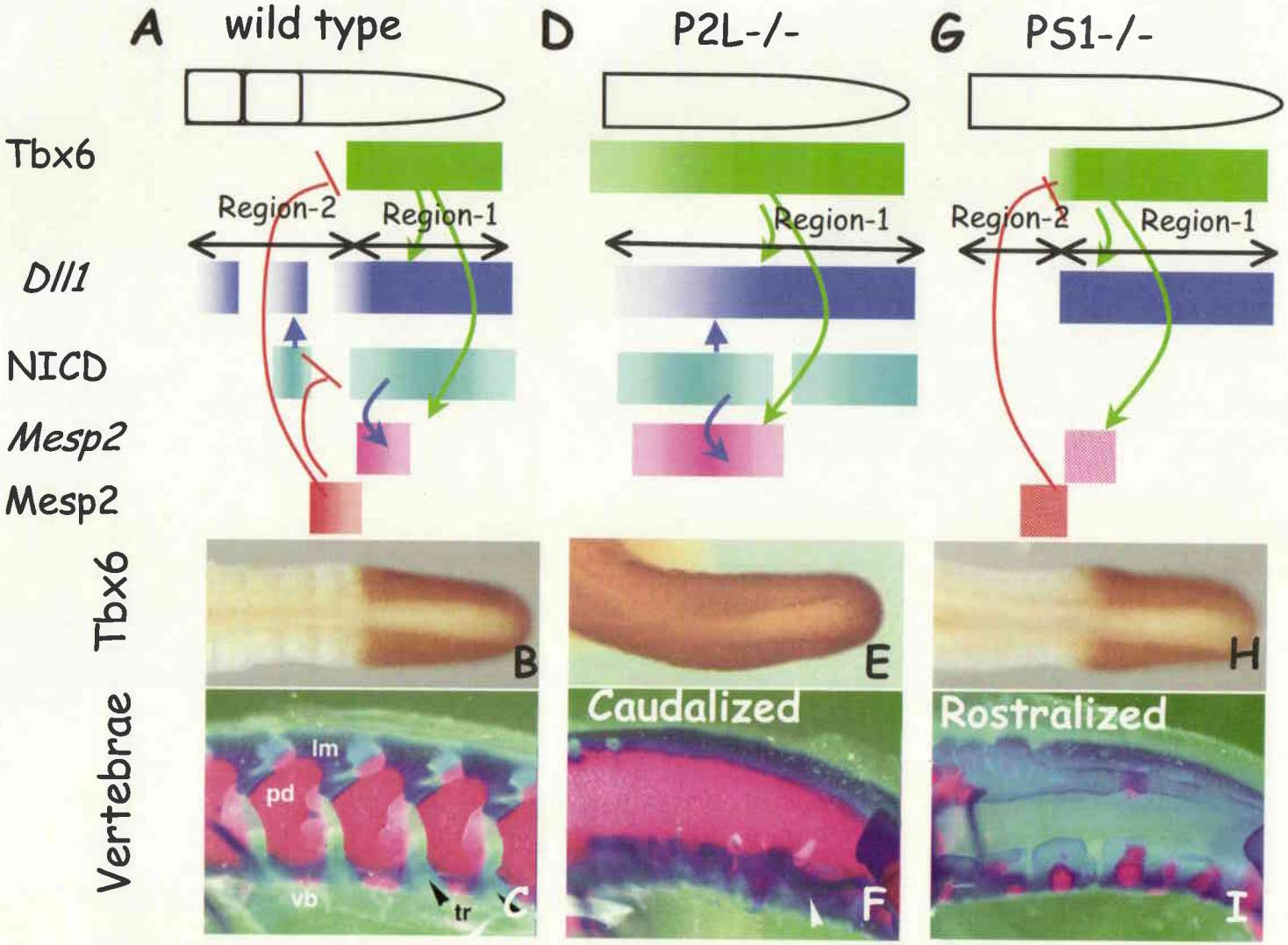

Figure 20. Proposed models of the genetic cascades leading to the establishment of RC patterning within a somite.

(A, D, G) Schematic representations of gene expression pattern among *Mesp2* (pink), Mesp2 (red), Tbx6 (green), *Dll1* (blue) and NICD (cyan) in the wild-type (A), Mesp2-null (D) or PS1-null mice (G). **(B-C, E-F, H-I)** Comparison of the expression patterns of Tbx6 protein and vertebral morphology in the wild-type (B-C), Mesp2-null (E-F) or PS1-null mouse (H-I). lm; lamina, pd; pedicle, vb; vertebral body.

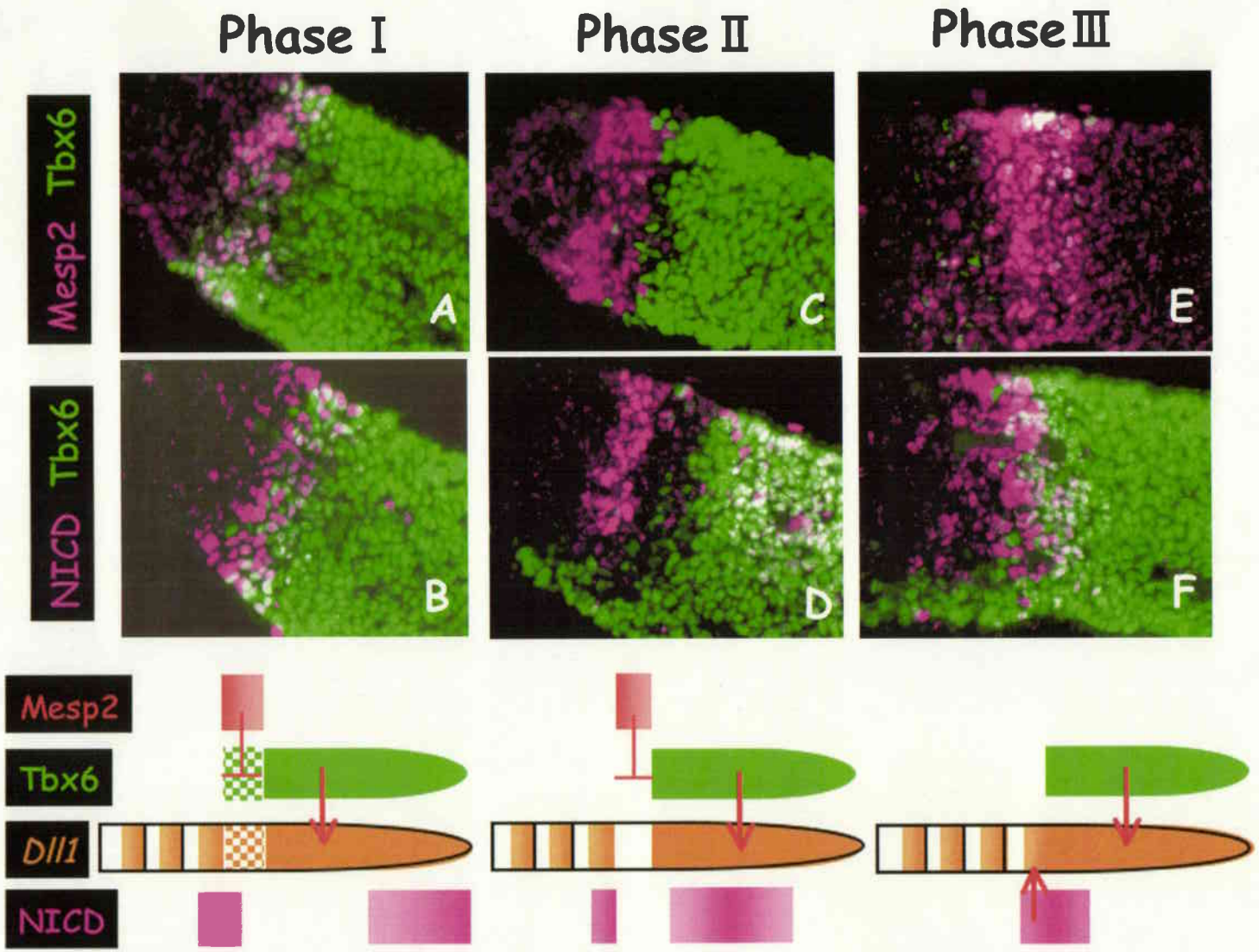

Figure 21. Proposed model for the mechanism that generates rostro-caudal patterning within a somite.

(A-F) The spatio-temporal relationship between Mesp2 and Tbx6 **(A, C, E)** and between Notch activity (NICD) and Tbx6 **(B, D, F)** during one